



室蘭工業大学

学術資源アーカイブ

Muroran Institute of Technology Academic Resources Archive



ニューラルネットワークを用いたFBGセンサの解析に関する研究

メタデータ	言語: eng 出版者: 公開日: 2018-06-06 キーワード (Ja): キーワード (En): 作成者: 袁, 莉莉 メールアドレス: 所属:
URL	https://doi.org/10.15118/00009643

Muroran Institute of Technology

Doctoral Dissertation

Study on analysis of FBG sensor
using neural network

Name: Lili Yuan

Supervisor: Assoc. Prof. Shinya Sato

Division of Engineering

Abstract

In recent years, fiber Bragg grating (FBG) sensors have attracted much attention because of their excellent properties and potential use in a wide range of applications. The excellent properties include small size, lightweight, remote sensing, wide bandwidth, immune to electromagnetic interference, lack of need for electrical power, and so on. These properties make FBG sensors play a more and more important role in monitoring and measuring the strain conditions of infrastructures.

However, since the conventional FBG strain sensors analyze reflected spectrum and measure the shift of reflected wavelength due to strain changes, a broadband light source, and an optical spectrum analyzer are indispensable devices, which make the measurement system large and expensive. In this research, we proposed a strain sensor system that measures strains from reflected power changes of FBGs. We used a laser diode as the light source and a power meter as the measurement device in the system, which make the FBG strain sensor system small-size and low-cost over to conventional FBG sensors. In addition, multipoint strain measurements can be implemented by using the time delay of reflected pulses of a series of FBG sensors with this measurement method. When there are two or more FBGs, an oscilloscope is used as the measurement instrument since it can perform multipoint measurements. In order to approximate the relationship between strains or temperatures and the reflected power, a feedforward neural network was used. This is because a feedforward neural network composed of three layers of an input layer, a hidden layer, and an output layer,

can approximate any function with high accuracy. Comparing with the results calculated by function fitting, accuracy was pretty improved by using a neural network.

First, the strain measurement experiment was conducted with only one FBG at room temperature. By applying strains to the FBG and measuring the changes in reflected power due to change in strains, the relationship between the strains and the power changes was obtained. Comparing the strains calculated by the function fitting and the strains calculated by the neural network, it was found that accuracy was improved by using the neural network. Then, a temperature compensation experiment was conducted using two FBGs connected in series based on the measurement method. In the experiment, one FBG was used for temperature measurement, and the other one was used for strain measurement. We heated both FBGs and applied strains to only one FBG in the experiment. In order to model the strain-temperature-power relationship of FBGs, the measured power of FBGs is used as the input layer of the neural network, while the strains and temperatures are used as the output layer. The temperatures and strains obtained using the neural network agree well with the actually applied temperature and strain in the experiment. In comparison with the strains and temperatures calculated using function fitting and that calculated by the neural network, it is found that the accuracy was greatly improved using the neural network. Furthermore, the output for the power other than the measured power was also correctly obtained. Therefore, not only the feasibility of the strain sensor system proposed in this research but also the data processing method using a neural network have been demonstrated by experimental results.

Contents

1. Introduction	1
1.1 General Background	2
1.2 Research Purpose	3
1.3 Dissertation Outline	4
2. Optical Fiber Sensor	6
2.1 Fundamental of the optical fiber	7
2.2 Fundamental of optical fiber sensors	9
2.3 Classification of optical fiber sensors	12
2.3.1 Optical Time Domain Reflectometry	13
2.3.2 Brillouin Optical Time Domain Reflectometry Sensor	13
2.3.3 Fiber Bragg Grating Sensor	15
3. Fiber Bragg Grating (FBG) Sensor	16
3.1 Outline of FBG	17
3.2 Measurement Principle of FBG Sensor	18
3.3 FBG Multipoint Measurement Principle and Problems	21
4. Neural Network	24
4.1 Outline of Neural Network	25
4.2 Components and Forms of Network	26
4.2.1 Neuron Model	27
4.2.2 Activation Function	29
4.2.3 Architecture of Neural Network	30
4.3 Backpropagation Method	32
4.4 Design of Neural Network	38

5. Experiments and Results	43
5.1 Experiment for Investigating the Characteristics of an FBG and Results	44
5.2 Results of the Characteristics Investigating Experiment using a Neural Network	50
5.3 Temperature Compensation Experiment and Results	55
5.4 Results of Temperature Compensation Experiment by a neural network	63
6. Conclusions	70
6. Conclusions	71
Acknowledgments	73
References	74

1. Introduction

1.1 General Background

In recent years, natural disasters are occurring frequently due to typhoons, earthquake and torrential downpours. Therefore, the realization of safe living by the advanced management of structures in the civil engineering and building fields is required. Thus, it is important to monitor the strain conditions in real time of social infrastructure such as roads, bridges and power facilities [1-3]. In addition, places where natural disasters are mostly harsh environments such as mountains, tunnels, and rivers, which are susceptible to erosion, lightning strikes, electromagnetic interference, and so on. Traditional electrical sensors are easily damaged by lightning, electromagnetic interference, etc., and are difficult to apply in these places. Optical fiber sensors can be used in these harsh environments without being affected because they have many unique advantages that are not available in traditional electrical sensors. The excellent properties of optical fiber sensors include compact size, lightweight, large bandwidth, the possibility of remoting sensing, anti-electromagnetic interference, low loss, good corrosion resistance, lack of need for power supply, and high sensitivity [4-10]. These characteristics enable optical fiber sensors to be widely used in aerospace technology, biosensors, smart robots, pressure sensors, railway monitoring systems and other engineering areas for sensing and monitoring as well as the structural health monitoring of buildings [11-23]. Fiber optic sensing converts measured external changes into changes in the characteristics of light propagating in the fiber, and these characteristics include intensity, phase, frequency, wavelength, polarization, and so forth [24-25]. There are several types of optical fiber sensors depending on the measurement principle. Among them,

the development of sensors using fiber Bragg grating (FBG) has been actively conducted [26-40]. This is due to the fact that in addition to the properties of optical fiber sensors described above, the FBG sensors have an excellent linear relationship with respect to temperatures and strains [41-43]. Therefore, they have potential applications in disaster-prevention sensing systems such as the collapse of tunnels, prediction of an earthquake as well as investigation of strains of infrastructures.

1.2 Research Purpose

Optical fiber sensors have been being actively studied as sensors for measuring physical quantities such as strains, temperatures, pressures, magnetic field, and so on. In particular, measurement methods using reflected light of fiber Bragg grating (FBG) are actively studied, and strain measurement sensors using FBGs are being studied for monitoring of structures in the field of building and civil engineering. However, since the conventional FBG strain sensors analyze reflected spectrum and measure the shift of reflected wavelength due to strain changes, a broadband light source and an optical spectrum analyzer are indispensable devices, which make the measurement system large and expensive. In addition, the measurement interval is long as the sweep time is slow, and it is also difficult to compensate for changes in the reflection spectrum of FBGs due to temperature changes. Thus, although the FBG sensors have reached a certain practical level, there are also some problems such as low of workability and scalability, high cost, which are limiting the development of FBG sensors to reach the spread level. In order to resolve the problems mentioned above and advance the spread level, instead of the

broadband light source and the optical spectrum analyzer, we developed an FBG strain sensor system using a laser diode as the light source and a power meter as the measurement device which can be found at a more affordable price. And, for data processing, we use a three-layer feedforward neural network to approximate the relationship of strains, temperatures, and the reflected power of FBGs. This method can miniaturize the experimental system and build it at low-cost. Furthermore, we conducted a temperature compensation experiment using the FBG strain measurement method reported here and the neural network.

1.3 Dissertation Outline

As described above, the introduction (Chapter 1) describes the general background, research purpose, and dissertation outline.

Chapter 2 presents an overview of optical fiber sensors. The concept, characteristics, and types of optical fiber sensors are described here.

Chapter 3 presents the outline of an FBG and the measurement principle of FBG sensors. Also, we described the strain measurement principle of the proposed FBG strain sensor in this study. In addition, the principle of multipoint measurement and the problems that will arise are also described in this chapter.

Chapter 4 is about the neural network, including the outline, components and form of network, and the backpropagation method. The design of neural network is also described for data processing.

Chapter 5 presents the experiment and experimental results. The experiment includes two parts. One is the strain measurement experiment, which is conducted using only one FBG, and this experiment is to investigate the strain characteristic of an FBG. The other one is a temperature compensation

experiment, which is conducted using two FBGs connected in series. In the experiment, one FBG is used for temperature measurement, and the other one is used for strain measurement. This experiment focuses on temperature compensation. The experiment and results are presented in this chapter, showing the feasibility of the proposed sensor system.

Finally, the conclusions drawn from this study are given in chapter 6.

2. Optical Fiber Sensor

2.1 Fundamental of the optical fiber

An optical fiber is a flexible, transparent fiber made of quartz glass or plastic for transmitting an optical signal, and is mainly used as a transmission line for optical communication [44-45]. Nowadays, in addition to optical communication, it has come to be used for various applications such as sensors, fiber lasers, high power light guides and the like. Along with this, fiber materials are becoming diversified, such as fluoride glass, chalcogenide glass, plastics as well as quartz glass. It is drawing attention to use as a sensor depending on its own characteristics and structure of the optical fiber. Optical fibers generally include a core and a cladding material that surrounds the core, and the index of refraction of the core is greater than that of the clad [46]. The cross section of the optical fiber is shown in Fig 2.1.1.

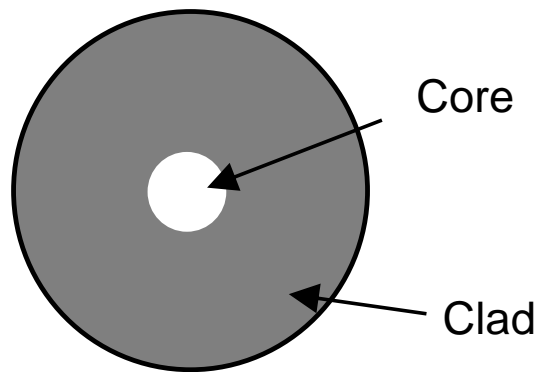


Fig.2.1.1. Structure of an optical fiber.

When light enters a medium with a small refractive index from a medium with a large refractive index, the light will be reflected and refracted at the boundary. We can change the incident angle of the light so that the light is totally reflected at the boundary, that is, there is only the reflected light but not the refracted light at the boundary. This phenomenon is called the total reflection. Total reflection is

also a necessary condition for transmitting light with an optical fiber. For this reason, the light could propagate in a state totally trapped inside the core of the optical fiber. Generally, the refractive index of the core is 1.47 and the refractive index of the clad is 1.46. The reflection and refraction of light at the boundary between materials with different refractive indices is shown in Fig.2.1.2 [47].

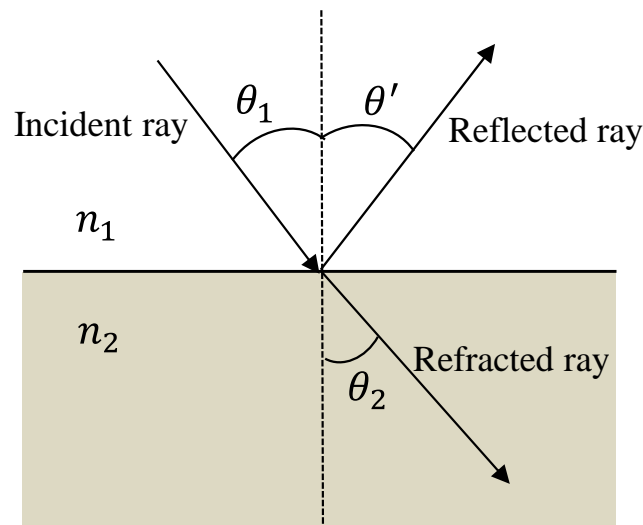


Fig. 2.1.2. Reflection and refraction of light.

The incident angle θ_1 and the reflection angle θ' are equal. According to Snell's law [48]

$$n_1 \sin \theta_1 = n_2 \sin \theta_2 \quad (2.1.1)$$

The n_1 and n_2 are the index of refraction of two different materials. Assume that the incident angle is θ_c when the incident light is refracted along the boundary surface, the value of $\sin \theta_2$ will become 1. From Eq. (2.1.1), we could obtain

$$\sin \theta_c = \frac{n_2}{n_1} \quad (2.1.2)$$

In the case of $\sin \theta_c \geq n_2/n_1$, the value of $\sin \theta_2$ will become larger than 1, the light will be completely reflected at the interface between the core and cladding,

which is the total reflection described above. And, the light can be confined in the core and transmit over a long distance using this property.

Fibers that support many propagation paths or transverse modes are called multi-mode fibers, while those that support a single mode are called single-mode fibers (SMF). Multi-mode fibers generally have a wider core diameter and are used for short-distance communication links and for applications where high power must be transmitted. Single-mode fibers are used for most communication links that are hundreds of kilometers or more. In this study, single-mode fibers are used to implement the experiments.

2.2 Fundamental of optical fiber sensors

Along with the development of optical fiber communication and optical fiber sensing technology, optical fiber sensors are rapidly developed. Prior to the development of optical fiber sensors, conventional electrical sensors were mainly used. However, electrical sensors are susceptible to environmental conditions because they measure changes in electrical signals to monitor changes in external strains, and use electrical wires transmit electrical signals. Furthermore, it is necessary to provide a power source in the measurement section for electric sensors. The electronic parts of the power supply and measurement section may be easily destroyed by short circuit or electromagnetic interference. In contrast to electrical sensors, fiber optic sensors transmit light signals using optical fibers and measure external strains using changes in light signals.

Nowadays, sensors are playing an extremely important role in production and living and are currently being studied to be more sensitive, more precise and more adaptable. Among many kinds of sensors, optical fiber sensors attract much

attention and research on optical fiber sensors is being conducted. Especially, optical fiber has properties as material such as intrinsic safety, non-inductive property and so on. Optical fiber sensor systems have been developed utilizing these characteristics. Optical fiber sensors are based on the principle that various physical phenomena are converted to optical signals via optical fibers, and are transmitted and processed. Currently, optical fiber sensors are used to measure almost all physical quantities. Those include pressure, temperature, speed, strain, load, gas concentration and so on.

The optical fiber sensor can be divided into two types depending on what role the optical fiber plays in the optical fiber sensor system [49]. One is to use the optical fiber only as a simple transmission path, and the other is to use the optical fiber itself as the sensor. When using an optical fiber only as a transmission line, as shown in Fig. 2.2.1, the light coming out of the optical fiber enters the sensor, and then the output light from the sensor enters the optical fiber again. The characteristics of light reaching the sensor from the light source through the optical fiber used as the transmission line change according to the external changes applied to the sensor. The characteristic changes are detected from the output of the light receiver. The other case that the optical fiber itself is used as a sensor is shown in the Fig. 2.2.2. When the physical quantity applied to the optical fiber from the external environment changes, the properties of the light propagating in the fiber also change. The characteristics of the light described here include the intensity, phase, wavelength, frequency, polarization, loss, etc. of the light. Since these characteristics change when an external change is applied to the optical fiber, it is possible to determine the external change applied

to the optical fiber from the change in the measured characteristic changes of light.

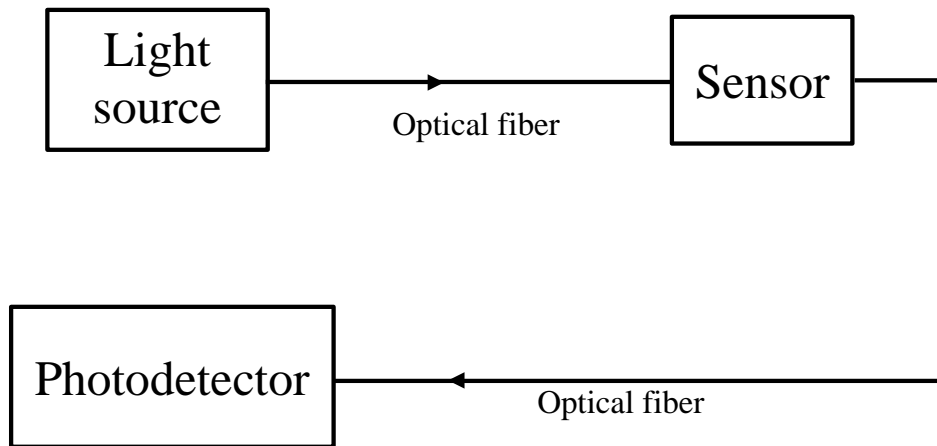


Fig. 2.2.1. Optical fiber used only as a transmission line.

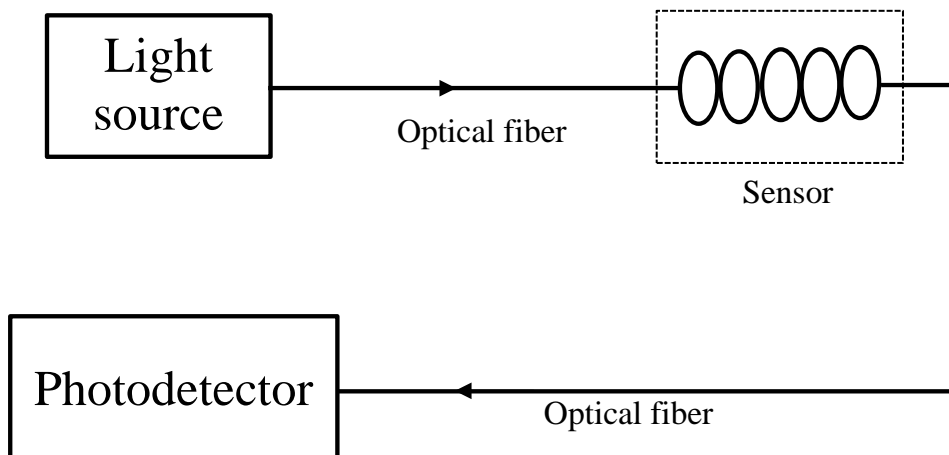


Fig. 2.2.2. Optical fiber itself used as the sensor.

In this study, we are conducting experiments using an FBG sensor of which the optical fiber itself is used as a sensor, so we will give some descriptions about optical fiber sensor of which the optical fiber itself is used as the measurement

part. This kind of optical fiber sensor has the following features and advantages.

- A) Small size, lightweight
- B) Flexibility
- C) Passive measurement unit
- D) High strength, durability, corrosion resistance
- E) Resistance to electromagnetic induction
- F) Distribution, quasi-distribution measurement

These advantages and features make the optical fiber sensor can be used where traditional electrical sensors cannot be used, such as the place where there is electromagnetic interference or the place where thunderstorms often occur.

2.3 Classification of optical fiber sensors

There are roughly three types of the optical fiber sensors when they are classified according to their constructions, particularly the way utilizing the optical fiber in the sensor system [50]. The first type is a sensor system in which the optical fiber is used as a transmission path of signal light. The multimode fiber is often used in this kind of optical fiber sensor system. The second one is an optical fiber probe sensor. The optical probe sensors perform the measurement by receive the light signal reflected from the objects to be measured. One of the great advantages of this type of sensor is that it can perform the measurement without contacting the objects to be measured. The third type is called a functional optical fiber sensor. Functional fiber sensors mainly use single-mode fibers in the systems. The working principle is to modulate and influence the transmission characteristics of the optical fiber according to the measured physical quantity, resulting in changes in the optical properties (intensity, wavelength, frequency,

polarization, etc.) of the light, thereby converting the measured physical quantity changes into modulated light signals. Using this, we can determine the changes in measured physical quantities from the optical signals received by the optical detector. As the FBG sensor used in this research is a sensor in which the optical fiber itself functions as a sensor, here we mainly explain some examples of the functional optical fiber sensors briefly.

2.3.1 Optical Time Domain Reflectometry

The Optical Time Domain Reflectometry (OTDR) is one of the optical fiber sensing technologies used to measure the backscattering light generated when light enters the fiber [51-52]. When the pulsed light is incident on the fiber to be measured, reflected light will be generated in a direction opposite to the incident direction. This phenomenon is known as backscattering and is used as the principle of optical fiber sensors.

The measurement principle of OTDR is to input optical pulses to the measurement optical fiber and measure the Rayleigh scattering light and the Fresnel reflection light returned from the measurement optical fiber with an optical receiver. From the time difference from the incidence of pulsed light until the scattering light or the reflected light returns, it is possible to find out the position where scattered light and reflected light occur. The OTDR can be used to measure fiber distance, transmission attenuation and loss, and fault location, and is therefore widely used in fiber measurement, construction, and maintenance.

2.3.2 Brillouin Optical Time Domain Reflectometry Sensor

As described in the previous section, various scattering lights are generated when the light entering the optical fiber propagates through the optical fiber. One

of the scattering light is called the Brillouin scattering light that depends on strain and temperature changes. That is, Brillouin scattering light shifts its frequency when temperature or strains are applied to the optical fiber.

The Brillouin Optical Time Domain Reflectometry (BOTDR) system is one of the fiber sensing methods for determining strains by measuring and analyzing Brillouin scattered light [53-55]. It uses the characteristic that the frequency distribution of the Brillouin scattering light shifts proportionally to the strains that applied to the optical fiber to carry out the measurement. The BOTDR sensing system uses a standard communication single-mode fiber as a sensing element. In addition, because it is also sensitive to temperature changes, a BOTDR system can provide simultaneous measurement of temperatures and strains, and can achieve continuous distributed measurement for several tens of kilometers in the longitudinal direction of the optical fiber.

By confirming in advance the characteristics of the optical fiber used for the measurement, and using the strain and temperature coefficient of the optical fiber as a result of the frequency shift of the measured Brillouin scattering light, the change in strain and temperature can be measured. If the sensor fiber is installed in a ring shape, the measurement can be continued by measuring from both ends even if a crack occurs in one place. In addition, it is possible to find the position where the strains occurred by measuring the time from the incidence of pulsed light until the Brillouin scattering light returns.

However, in order to achieve high-precision measurement, the demand for the light source in the BOTDR system is strict, and generally a BOTDR system requires a light source with high power, stable output, and narrowband. Moreover,

since the Brillouin scattering light signal returned to the incident end is weak, it is relatively difficult to perform the measurement. It is necessary to perform the averaging process, and a measurement may take tens of seconds to tens of minutes. Therefore, it takes a long time to perform a complete measurement, and the real-time performance is not good enough to perform dynamic measurement.

2.3.3 Fiber Bragg Grating Sensor

A fiber Bragg grating (FBG) is an element constructed by forming a periodic refractive index modulation in the core of a short segment of optical fiber. When the light enters the FBG, the particular wavelengths of light will be reflected and all the others will be transmitted. With the rapid development of fiber Bragg grating (FBG) sensing technology recently, FBG sensors have been widely used in sensing and monitoring in various engineering fields, such as building structure health monitoring, aerospace technology, pressure sensors, electric power industry, Intelligent robots, railway monitoring systems, etc. The detailed description of FBG sensors will be presented in Chapter 3.

3. Fiber Bragg Grating (FBG) Sensor

3.1 Outline of FBG

A fiber Bragg grating (FBG) is an element constructed by forming a periodic refractive index modulation in the core of an optical fiber along the direction of propagation. An FBG will reflect a particular wavelength called the Bragg wavelength (λ_B) and transmit the other wavelengths when light enters the FBG. The Bragg wavelength also has a feature that it varies with mechanical strains and ambient temperature changes applied to the optical fiber [42-44]. This leads to their utility as temperature and strain sensors. Figure 3.1.1 shows the schematic diagram of a FBG.

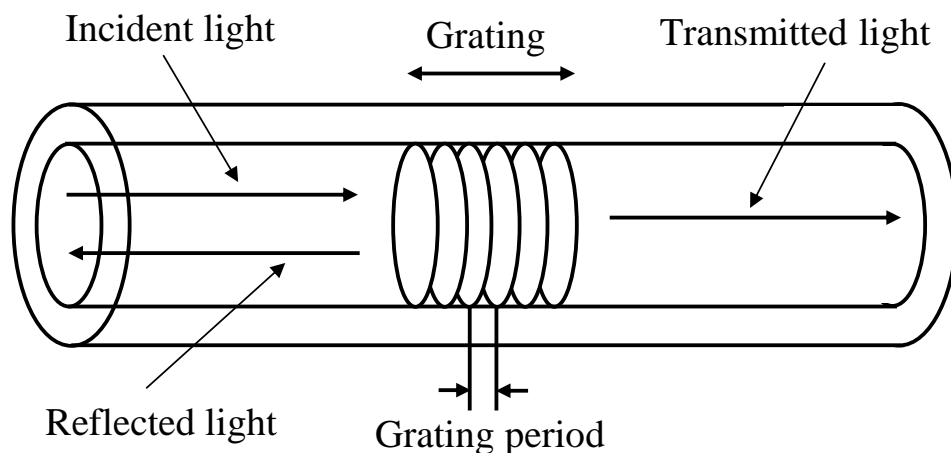


Fig. 3.1.1. FBG sensing principle.

When the light output from the light source is incident on the FBG, the reflection of the grating that periodically changes the refractive index interferes in a direction in which they strengthen each other only for a specific Bragg wavelength. As a result, the FBG reflects only the Bragg wavelength and transmits all other light components. The Bragg wavelength can be expressed by the equation given by

$$\lambda_B = 2n_{eff}\Lambda \quad (3.1.1)$$

where n_{eff} is the effective refractive index of the grating in the fiber core, and Λ is

the grating period [56-59]. From Eq. (3.1.1), we find that the Bragg wavelength is a function of the refractive index and the period. When the FBG is stretched or heat is applied to the FBG, the grating period Λ will be stretched and n_{eff} also changes at the same time resulting in a shift in the Bragg wavelength, which makes it possible to detect the amount of strains or temperature changes by measuring the shift amount of the Bragg wavelength.

Fabrication of FBGs benefits from the photosensitivity in optical fibers, as a small amount of germanium is added to the optical fiber core in order to increase the refractive index. The photosensitivity means that exposure to ultraviolet radiation induces a permanent change in refractive index. The most common method for fabricating FBGs is phase mask processing [58], i.e. irradiating light having periodically distributed intensity on the photosensitive core and locally changing the refractive index of the optical fiber according to the intensity of the light irradiated to fix the state.

3.2 Measurement Principle of FBG Sensor

As described above, FBGs are sensitive to temperature and strains. When the external temperature or strains applied to the FBG changes, the center wavelength of the reflection spectrum of the FBG shifts [60-61]. Therefore, in the conventional FBG sensor system, strains and temperature are obtained by measuring the shift amount of the center wavelength of the reflected spectrum of the FBG. However, since the change of the center wavelength is measured, the sensor system requires a broadband light source and a spectrum analyzer, which makes the sensor system becomes large and expensive. In addition, the measurement interval becomes long as the sweep time is slow, making it difficult

to compensate for the change in the reflection spectrum of the FBG caused by temperature changes. Thus, although the FBG sensors have reached a certain practical level, there are also some problems such as low of workability and scalability, high cost, which are limiting the development of FBG sensors to reach the spread level.

In order to solve the problems described above and advance the spread level, we developed a sensor system that determines strains applied to the FBG by measuring the reflected power of the FBG. Instead of broadband light source and a spectrum analyzer, we used a laser diode which is a narrow-band light source as the light source, and a power meter as the measurement device. As a result, the sensor system can be small size and be constructed at low cost. Furthermore, the reflected power is measured in the experiment so that the light source and the measurement instrument are placed at the same direction end, reducing the operational difficulties.

The reflected power of an FBG can be expressed by the product of the reflectivity of the FBG and the optical power of the laser diode light source, and the measurement principle of the reflected power of an FBG is shown in Fig. 3.2.1 [36]. The reflected power of an FBG changes owing to the change in the reflectivity of the FBG, as the width of the laser diode light source used in the experiment is constant. Fig. 3.2.2 [36] shows the shift of the reflected spectrum of the FBG caused by strain changes. From Fig. 3.2.2, it can be seen that the reflected spectrum will shift towards the longer wavelength side when strains are applied to an FBG.

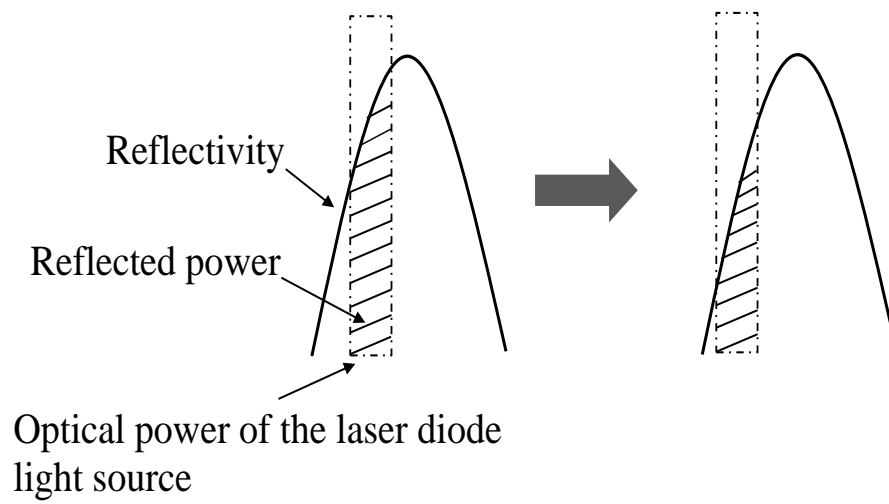


Fig. 3.2.1. The measurement principle of the reflected power of an FBG.

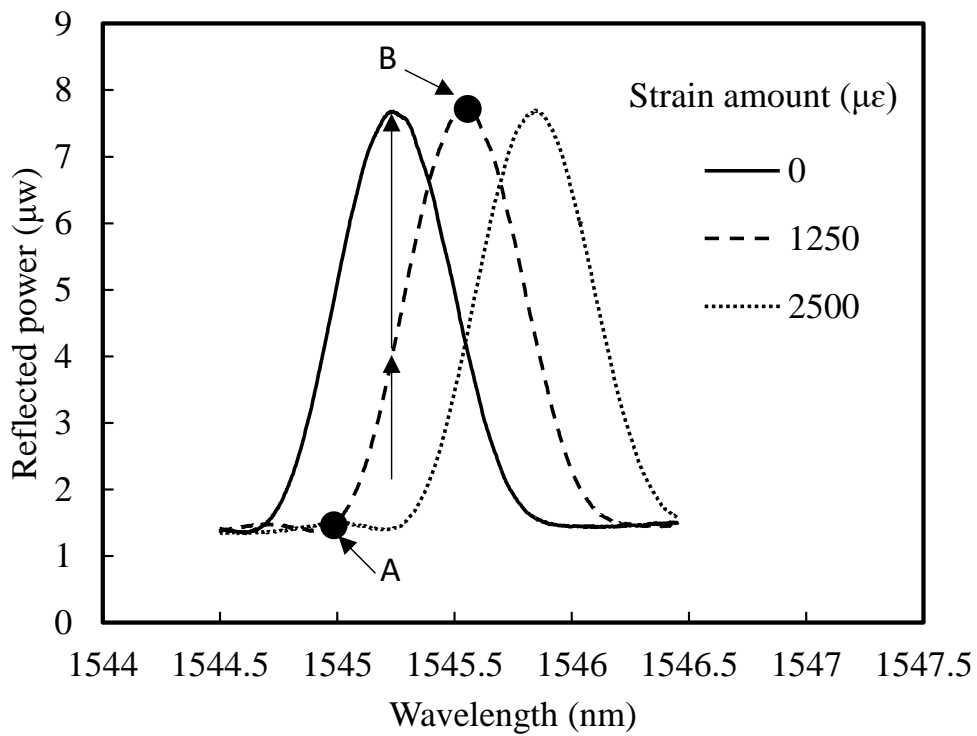


Fig. 3.2.2. The shift of the reflected spectrum of an FBG.

From Fig. 3.2.2, we observe that the reflectivity of FBG the monotonically varies between points A (minimum point) and B (maximum point). Therefore, we can limit the measurement range to this monotonically changing interval so that each

value of the measured reflected power corresponds to a certain strain value. Since the reflected spectrum of the FBG is symmetrical about the center wavelength, the measurement range can also be limited to the monotonically changing range of the other side. Since the light source used in the experiment remains unchanged, it can be seen from Fig. 3.1.1 that the area surrounded by the FBG reflected spectrum and the laser diode light source, that is, the reflected power of the FBG, becomes smaller. Based on this principle, we have developed an FBG sensor system that determines the strain by measuring the reflected power of the FBG.

3.3 FBG Multipoint Measurement Principle and Problems

In practical applications, multiple FBG sensors are required for both multipoint strain measurement and temperature compensation experiments as shown in Fig. 3.3.1. In this study, the temperature compensation experiment is also conducted based on the experimental system shown in Fig. 3.3.1.

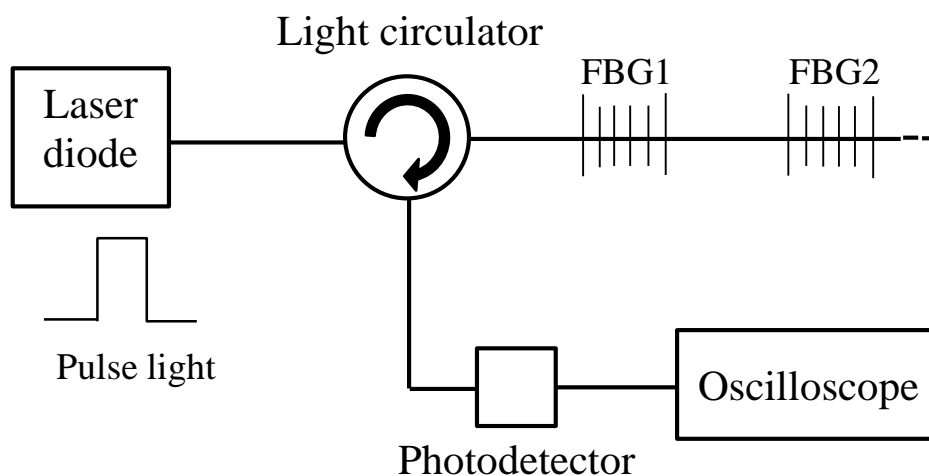


Fig. 3.3.1. Multipoint measurement experiment system.

We can see that the FBGs are connected in series. A laser diode which emits pulse light is used as the light source, while an oscilloscope is used as the measurement device which still makes the experiment system remain small size. The photodetector is used to convert the light signals into electrical signals so that the signals can be detected by the oscilloscope. When the pulse light enters into the FBGs via the light circulator, it will be reflected by the FBGs. The reflected pulses from each FBG measured by the oscilloscope can be expressed by Fig. 3.3.2.

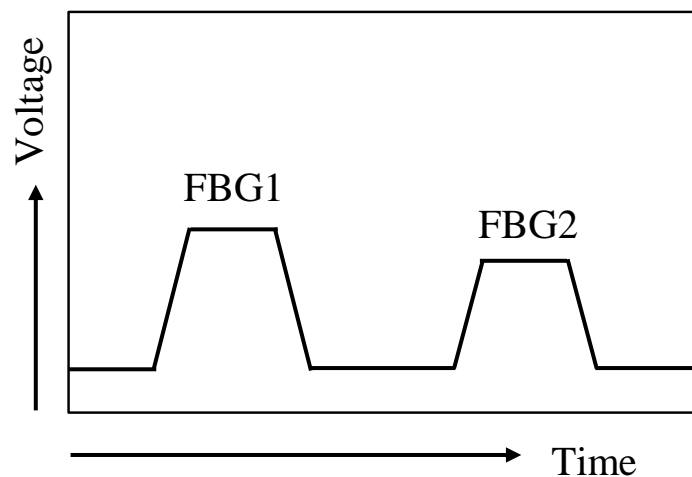


Fig.3.3.2. Reflected light of each FBG.

This is conducted by using the time delay of reflected pulses from each FBG sensor with the measurement principle we developed. In addition, to prevent the reflected pulses from the FBG sensors overlap, we must use long enough fiber to connect the FBGs. Therefore, the time it takes to reach the measurement device is different as the optical path is different. This is also the cause of the multipoint measurement. The time T for a round-trip to a FBG can be expressed by

$$T = \frac{2L}{c/n_1} \quad (3.3.1)$$

Here, the L is the length between two FBGs, the c is the light speed in vacuum, and the n_1 is the refractive index of glass. The minimum length L' between two FBGs which make sure the reflected pulses light not overlap can be obtained when $s = T$. The minimum length L' can be calculated by

$$L' = \frac{cs}{2n_1} \quad (3.3.2)$$

Here, the s is the sum of the pulse width and the edge time.

However, when the number of series-connected FBGs is increased to 3 or more, the third FBG will be affected by a lot of conditions. To be understood easily, here we call the FBG closest to the light source FBG1, followed by FBG2 and FBG3, respectively. First, when the temperatures or strains of FBG1 and FBG2 change, the light transmitted through FBG1 and FBG2 will change, that is, the light entering FBG3 changes too. In this way, even if the strains and temperatures of the FBG 3 do not change, since the light entering the FBG3 changes, the measured reflected light of FBG3 will change too.

In addition, when the temperatures and strains applied to the FBG3 change, the reflected light of the FBG3 also changes. As a result, the parameters that cause the reflected light of the FBG3 to change will increase, and it will become very difficult to obtain the strains applied to the FBG3 using the function fitting. Therefore, as a solution, we decided to use neural networks for data processing to determine the strains applied to FBG3 which are the amount of strains after removing other influences. The detailed description of the neural network will be introduced in Chapter 4.

4. Neural Network

4.1 Outline of Neural Network

The neural network is a mathematical model for information processing that simulates the human brains. When a neural network is used as a method in engineering, it must be called an artificial neural network. The study of neural network information processing began with the proposal of neuron model by Warren S. McCulloch and Walter Pitts in 1943 [62]. In their study, they described the concept of neurons which are single cells present in cellular networks that accept inputs, process their inputs and generate outputs. Neural networks can effectively approach a wide range of applications because they have the ability to deal with non-linear problems [63-65]. And, they are networks constructed by mutually connecting artificial elements simulating nervous system cells (neurons) of a living body, and mainly a neural network has three great features [66].

The first feature is "nonlinearity". This is very important. It is because of the strong nonlinear characteristics of the network that we can use a neural network to approximate any function with high accuracy. If a linear activation function is used in the system, then no matter how complex the network is, the output we obtain is just a linear transformation of the input, as if the neural network contains only one layer. This is because the linear activation function has limited learning ability. However, in practical applications, we will encounter many problems which are non-linear. Nonlinearity also means that the output is not a linear combination of inputs, but can establish a non-linear mapping between inputs and outputs.

The second feature is "parallelism". Neural networks are large-scale systems that deal with information processing in parallel, and a theoretical system for systematically grasping parallel operation has been established. It becomes

possible for high-speed processing by taking advantage of this feature.

The third feature is "learning ability", which is also considered to be the greatest attraction of neural networks. Learning ability is the ability to automatically create the necessary functions based on the provided examples (training data). This ability applies to problems that traditional methods cannot solve. With this ability, we can get the relationship between the inputs and outputs only by providing the input and the corresponding output data to the neural network.

4.2 Components and Forms of Network

Neural networks are constructed using artificial elements that simulate neurons of human brains. Since the behavior of actual neurons is very complicated, it is impossible to reproduce all the functions of the neurons of living bodies. Thus, when constructing a neural network, we usually use a neuron model that extracts specific functions so as to be easy to do in practice. That is, we express the function of the neurons by a mathematical expression. Before we explore how neural networks work, we must first understand the working methods of neurons that make up a neural network. In other words, when inputs are provided to a neuron, in what kind of way and what kind of outputs it will give. And based on our own experimental data, we have to decide the model of neurons to be used in our study. When deciding the model of a neuron, it is generally considered from two aspects [66]. The first one is whether the neuron always gives the same output when the same input is provided to the neuron. The other one is that the output of a neuron takes the two values of 0 and 1, or a continuously changing analog value. In our experiment, the reflected power of the FBG is determined when the temperatures or strains are determined. Moreover, as the temperatures

or strains change, the reflected power of the FBG changes continuously. Therefore, the neuron model we use must have a determined output for the same input. And the output value of the neuron must be a continuous analog value. The neuron model and the activation function used are described as follows.

4.2.1 Neuron Model

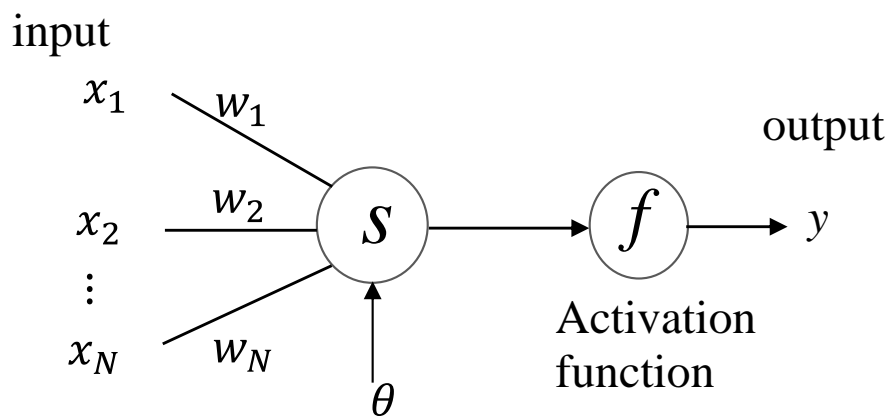


Fig. 4.2.1. Neuron model.

The neuron model is shown in Fig.4.2.1. The $\{x_1, x_2 \dots x_N\}$ represent the signal input that the neuron receives from other neurons. And, $\{w_1, w_2 \dots w_N\}$ are the weights for each input. The y represents the output signal from the neuron. The output y can be calculated using the equations [66] as follows:

$$s = \sum_{n=1}^N w_n x_n \quad (4.2.1)$$

$$y = f(s - \theta) \quad (4.2.2)$$

As described above, neurons composing of a neural network is elements that simulate neurons of living bodies. Thus, the s is an amount corresponding to the intracellular potential of the living body neurons. And, θ represents the threshold of whether the neuron is excited or not.

Again, we can observe that the neuron model contains two kinds of parameters, the weight, and the threshold. When we use neural networks composed of neurons for learning, the neural networks need to modify the values for both the weights and the threshold to perform the learning so that the difference between the output of the neural network and the target output that we expect become smaller. So, the smaller the number of parameters, the easier it will be to modify the parameters. Therefore, in practical applications, a small change is always made to the model of the neuron, that is, treat the threshold as one of the inputs [67]. That is, an input x_0 , the value of which is 1, is added to the inputs, and its weight w_0 is set to $-\theta$. In this way, the model can be rewritten as shown in Fig. 4.2.2.

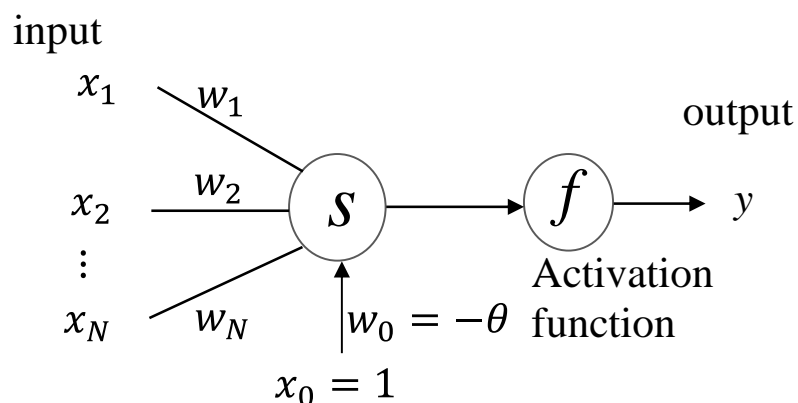


Fig. 4.2.2. Treat threshold as one of weights.

When learning, we can modify only the weights of the neurons. Since the threshold of the neuron is treated as one of the weights, the threshold value is modified at the same time. The intracellular potential s and the output y of the neuron can be expressed by the following equation [67].

$$s = \sum_{n=0}^N w_n x_n \quad (4.2.3)$$

$$y = f(s) \quad (4.2.4)$$

4.2.2 Activation Function

When we calculate the output of a neuron using the intracellular potential s calculated by Eq. (4.2.3), we need to substitute the s into the activation function f for calculating the output. A function called the sigmoid function is usually used as the activation function which is a nonlinear function of neurons. The sigmoid function is shown in Fig. 4.2.3, and its equation is expressed as Eq. (4.2.5) [66].

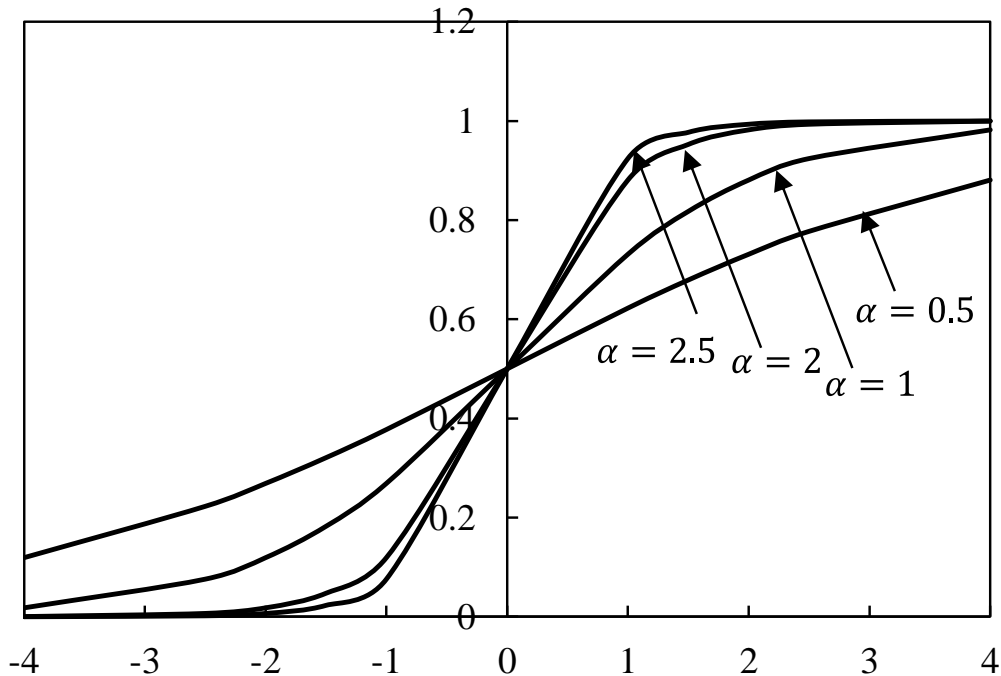


Fig. 4.2.3. Sigmoid function.

$$\text{sigmoid}(g) = \frac{1}{1 + e^{-\alpha g}} \quad (4.2.5)$$

Here, α is a coefficient called gain, and g represents the value on the horizontal axis. The sigmoid function is an important function representing the input/output characteristics of neurons. The output of the sigmoid function is continuous and known as a monotone function of the input. In addition, the derived function of

the sigmoid function is very easy to calculate, and can use its own to represent its derived function. The derived function of the sigmoid function is

$$\text{sigmoid}'(g) = \frac{\alpha e^{-\alpha g}}{(1+e^{-\alpha g})^2} = \alpha \text{sigmoid}(g)(1 - \text{sigmoid}(g)) \quad (4.2.6)$$

This is used in the Backpropagation method which will be introduced later. We can also know that the function value is in the range of $0 \leq y \leq 1$, this ensures that the data is not easily divergent during transmission. Continuous output can be obtained by using this function when calculating the output y from s . Also, as shown in Fig. 4.2.3, the sigmoid function approaches the step function if the gain of the sigmoid function is increased. Conversely, when the gain is larger than 0 and sufficiently smaller than 1, the sigmoid function cannot be used either. Thus, it is necessary to pay attention to these two points. Therefore, when setting the initial value for the gain, it must not be too large or too small. Using the sigmoid function as the activation function, Eq. (4.2.2) and (4.2.4) can be rewritten as [66]

$$y = \text{sigmoid}(s - \theta) \quad (4.2.7)$$

$$y = \text{sigmoid}(s) \quad (4.2.8)$$

4.2.3 Architecture of Neural Network

A neural network is connected by the neuron-like elements as described in the previous section. Also, it can be divided into two types when classified from the structure of the network [68]. One is called a feedforward neural network, and the other is called a recurrent neural network. A neural network consists of one input layer, several hidden layers, and one output layer.

(1) Feedforward neural networks

A feedforward neural network is a biologically inspired classification algorithm.

An example of a feed-forward network is shown in Fig. 4.2.4, from which we can find that a feed-forward network allows signals to travel one way only, from input to output.

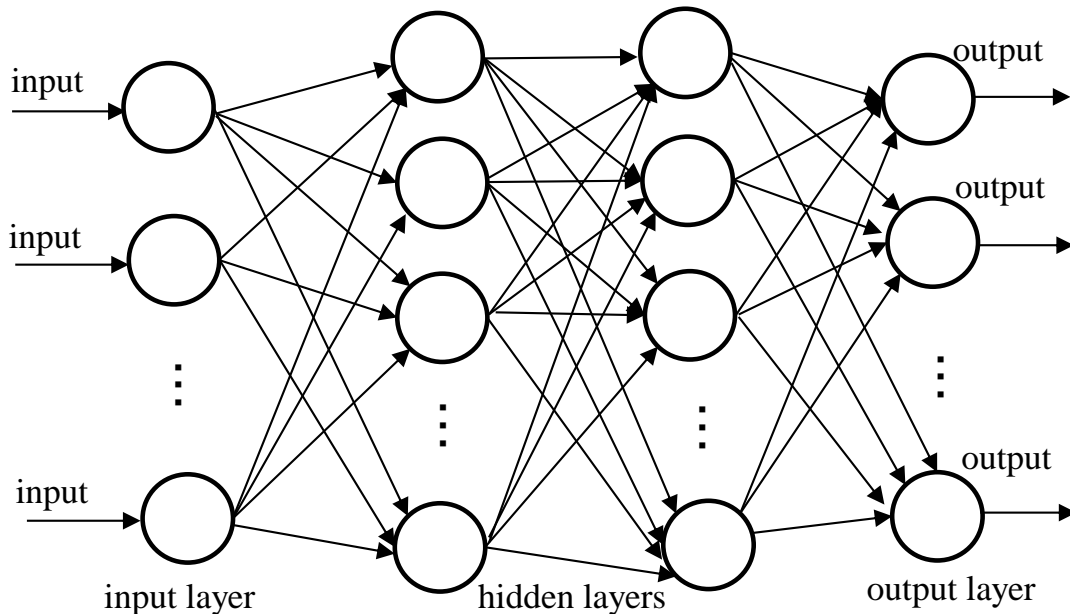


Fig. 4.2.4. An example of a feedforward neural network.

It consists of a number of simple neuron-like elements composed of layers. Every element in a layer is connected with all the units in the previous layer. Each connection may have a different weight. There is no feedback between layers. In this case, when the values of the elements of the input of the network are determined, the values of the elements can be determined one after another toward the output.

(2) Recurrent neural networks

Different from the feedforward neural networks, the flow of the output signal of recurrent neural networks is bidirectional, that is, when determining the values of neurons of the input layer, the values of neurons of the output layer must also be considered. An example of a recurrent neural network is shown in Fig. 4.2.5, from

which we can find that signals can be exchanged between arbitrary neurons.

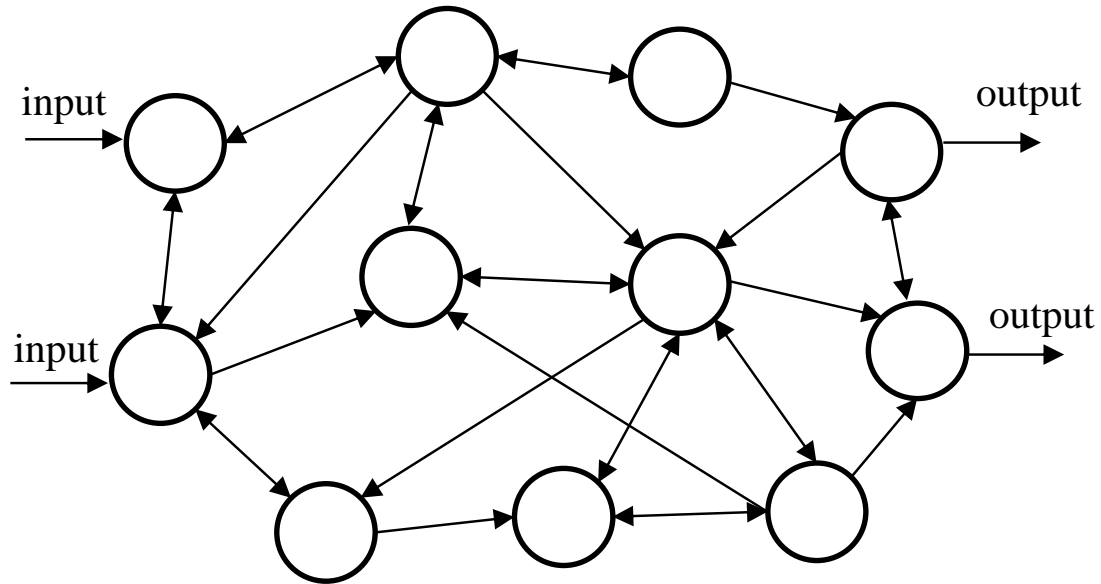


Fig. 4.2.5. An example of a recurrent neural network.

Recurrent neural networks are more powerful than feedforward neural networks and can get extremely complicated. They are dynamic, and the states are changing continuously until they reach an equilibrium point. They remain at the equilibrium point until the input changes and a new equilibrium needs to be found. It seems to be difficult, but because the output is decided after a certain amount of time lag with respect to the input, this cycle of circulation can be solved.

4.3 Backpropagation Method

The error backpropagation method was proposed by Rumalhart, Hinton, and Willians in the 1980s and is a convenient algorithm to learn a neural network. In particular, the error backpropagation method is one of the learning methods of feed-forward neural networks, and is currently being studied and used most

aggressively in neural network algorithms [69-70].

As shown in Fig. 4.3.1, there are inputs (x_0, x_1, \dots, x_N) and target outputs (t_0, t_1, \dots, t_M) , while outputs (y_0, y_1, \dots, y_M) are calculated by the neural network. In order to make the network output (y_0, y_1, \dots, y_M) infinitely close to the target output (t_0, t_1, \dots, t_M) , we use backpropagation method to adjust the network parameters, that is, the threshold and weights, thus changing the relationship between inputs and outputs of the neural network. Fig. 4.3.2 [67] shows this process.

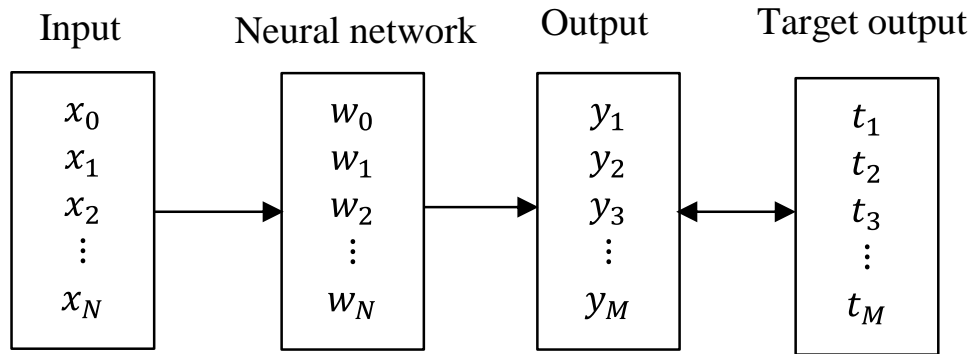


Fig. 4.3.1. Diagram of neural network learning.

Input (x_0, x_1, \dots, x_N) and target output (t_0, t_1, \dots, t_M) are the specified input-output relationship, which are also the learning goals. When inputting (x_0, x_1, \dots, x_N) to the neural network, the neural network will give an output (y_0, y_1, \dots, y_M) . The input-output relationship of the network is expressed by function $(y_0, y_1, \dots, y_M) = F(x_0, x_1, \dots, x_N)$. The error back propagation method gives a procedure for defining the parameters of the neural network so that the function $(y_0, y_1, \dots, y_M) = F(x_0, x_1, \dots, x_N)$ could realize the specified input / output relationship. The error evaluation function E represents the error between the target out t and the output y of the neural network, which is given as [67]

$$E = \sum_{m=1}^M |y_m - t_m|^2 \quad (4.3.1)$$

Give random initial values to the parameters, then modify the parameters repeatedly to make the error evaluation function E be as small as possible. The data used for parameter determination are called training data. When the parameters are determined, the relationship between the specified inputs and outputs could be determined too. In addition, the original purpose of learning is to acquire the ability to give outputs correctly even for inputs other than training data.

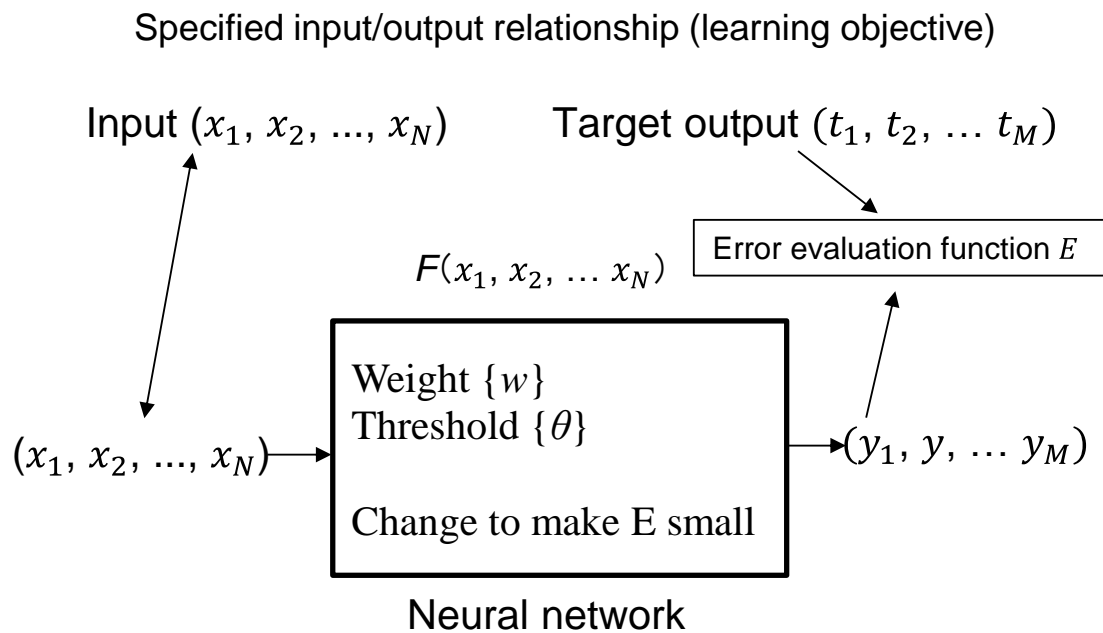


Fig. 4.3.2. Framework of error backpropagation method.

Therefore, in the error back propagation method, when an input is given to the network, the weights and thresholds of each neuron of the network are modified so that the output to that neural network matches the target output. As described before, the threshold is treated as one of the weights.

We will explain the feedforward neural network shown in Fig. 4.2.4 as an example. For the neurons constituting the neural network, we use the neuron

model described in section 4.2. That is, the threshold is treated as one of the weights. Therefore, it is enough to modify only the weights of each neuron.

In this research, we analyze experimental data using a three-layer feedforward neural network, so here we explain the error backpropagation method based on a feedforward type neural network which is a 2-input and 2-output feedforward neural network as shown in Fig. 4.3.3. In the error backpropagation method, the weights of each neuron are minutely modified each time the training data is given.

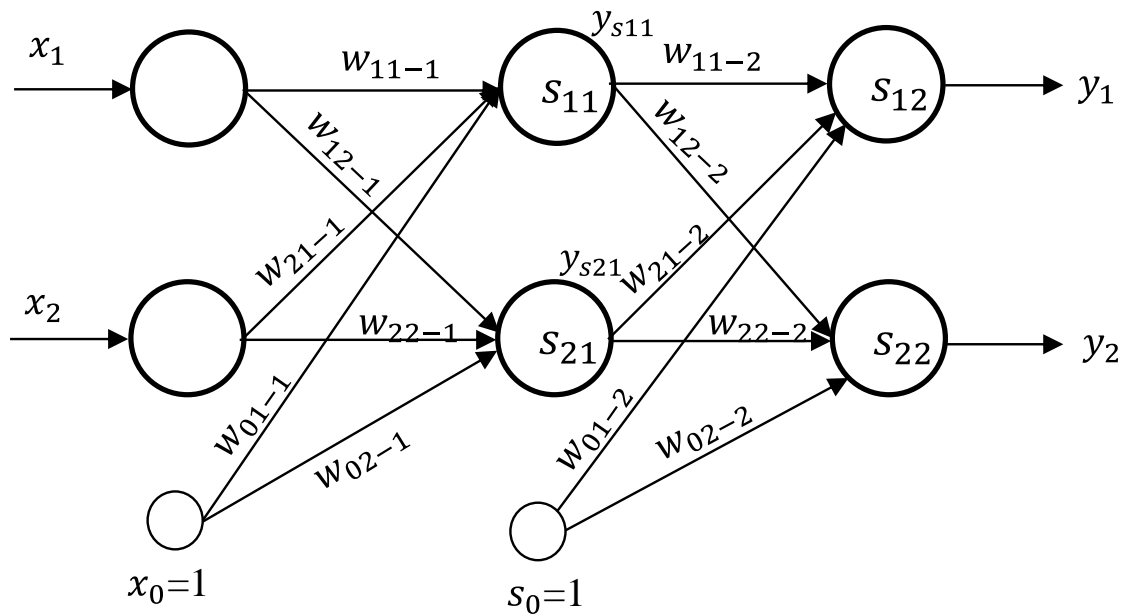


Fig.4.3.3. Forward mode of error backpropagation method.

The first step is to calculate the actual output y of the neural network when the input x is given to the neural network. The step for calculating the actual output y is also called the forward mode as shown in Fig. 4.3.3. Here, the x_1 and x_2 are the inputs given to the neural network, while the y_1 and y_2 are the outputs of the neural network. The w represents the weights. The threshold of

each neuron is treated as one the weights. There are elements that always output a value of 1 in each layer, and the weights of these elements are $-\theta$.

Before starting the learning, we need set each weight a random initial value to break the symmetry. Then provide the input and the target output to the neural network as the training data, which are used to determine a set of weights. This set of weights could correctly represent the relationship between the input and the target output. The actual output of the neural network could be calculated using the equations as follows:

$$S_{11} = w_{11-1}x_1 + w_{21-1}x_2 + w_{01-1}x_0 \quad (4.3.2)$$

$$y_{s11} = \text{sigmoid}(s_{11}) \quad (4.3.3)$$

$$y_1 = w_{11-2}y_{s11} + w_{21-2}y_{s21} + w_{01-2}S_0 \quad (4.3.4)$$

The y_{s11} and y_{s21} are the output of the neurons in the hidden layer. As the outputs form the inputs for the next layer, all the outputs could be determined for each layer from the input layer to the output layer. Here, we only gave the calculation for y_1 , and the output y_2 can be obtained in the same way.

After calculating the outputs of the neural network, the difference $y_i - t_i$ between the actual outputs of the neural network and the target output could be obtained easily. Then the difference between the actual outputs of the neural network and the target output are given to the neural network in the backward mode to modify the weights. Fig.4.3.4 shows the backward mode of the error back propagation method.

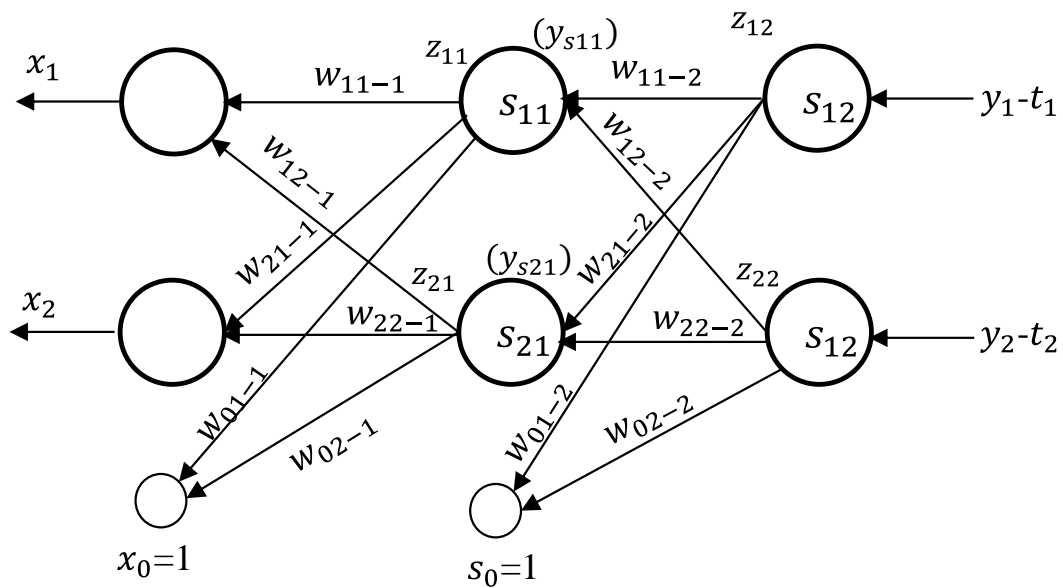


Fig. 4.3.4. Backward mode of error back propagation method.

In the backward mode, the signals travel in opposite direction. The difference between the actual outputs of the neural network and the target output are given to the network shown in Fig. 4.3.4. They are the inputs for the backward mode. The y_{s11} and y_{s21} are the outputs of neurons in the hidden layer calculated in the forward mode. The z represents the outputs of each neurons in the backward mode as shown in Fig. 4.3.5 [67], and it can be calculated using Eq. (4.3.5).

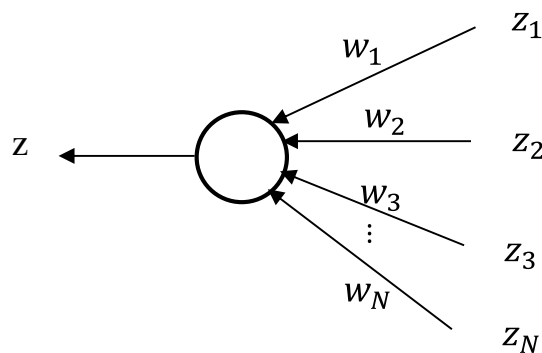


Fig. 4.3.5. Neuron model in backward mode.

$$z = \text{sigmoid}'(g) \sum_{n=1}^N w_n Z_n \quad (4.3.5)$$

Here, the $\{Z_1, Z_2, \dots, Z_N\}$ are the inputs to the neuron, and $\{w_1, w_2, \dots, w_N\}$ are the weights corresponding to the inputs. We can know that the derived function of the sigmoid function is used to calculate the outputs of neurons in backward mode.

After the output z of each neuron is calculated, the weights are modified using

$$w_{ij-(l+1)} = w_{ij-(l+1)} - \rho y_{sil} Z_{j(l+1)} \quad (4.3.6)$$

Here, the ρ is a small positive number that determines the degree of weight correction during learning, and l represents the number of the layer in which the neurons are, and the $w_{ij-(l+1)}$ represents the weight connecting the neuron of number i in layer l and the neuron of number j in layer $(l + 1)$. Here, we used a feedforward neural network with only two inputs and two outputs for explain the backpropagation method. However, the problems to be solved may be very complicated, with hundreds of inputs.

4.4 Design of Neural Network

The greatest feature of a neural network is learning ability, that is, the neural network can learn from examples. Whatever input is given to the network, through a series of calculations, it will give an output very close to the target output corresponding to the given input. In order to obtain the output that we want, we have to design the neural network properly [71-73].

When inputs are given to the neural network, the outputs will be obtained in the forward mode. Basically, an error occurs between the output obtained from the network and the target output. To minimize the error, the weights w_{ij} of the network are adjusted in the backward mode. As mentioned earlier, the adjustment

of the weights is performed using the back propagation.

As we learned about the function approximation ability of the feedforward type neural network, we can approximate any function with high precision using a feedforward type neural network, which consists of three layers of one input layer, one hidden layer, and one output layer [66]. However, in order to improve the accuracy of function approximation, the number of neurons in the hidden layer has to be increased. Also, as we can see from a variety of successful examples, most problems can be obtained with sufficiently high accuracy with a three-layer feedforward neural network. Therefore, in this research, we also decided to use a feedforward type neural network consisting of one input layer, one hidden layer, and one output layer. Although a three-layer neural network seems simple, designing a successful network is by no means easy. In order to obtain the output that is expected, we must devise properly the design of the network.

Before designing a neural network, the outputs and inputs of the neural network must be decided. In other words, what kind of outputs we would like to obtain using the neural network, and what kind of inputs that should be chosen to reach that goal. Once the outputs and inputs are determined, the number of neurons for input layer and output layer could also be determined. In the research, the strains and temperature applied to the FBGs are the expected values that we would like to obtain, so these are outputs of the network. For the desired outputs, the measured values of the reflected power of FBGs are given to the network as inputs of the neural network.

In general, we will either increase the number of neurons in the hidden layer or increase the number of hidden layers to achieve good learning results. As

mentioned earlier, in order to improve the accuracy of approximation, the number of neurons of the hidden layer has to be increased. Also, the hidden layer has a feature detection function, which responds to specific features of input. And, if the number of neurons in the hidden layer is not appropriate, it tends to locally minimize, so it is very important for the research on how to determine the number of neurons in the hidden layer. When the number of neurons in the hidden layer is too small, the learning time becomes faster, but the performance of the network is bad and it is not possible to grasp the feature of the input. In contrast, when the number of neurons in the hidden layer is too large, the learning time becomes very long and overfitting occurs, and an optimum solution cannot be obtained. So far, various methods have been reported to determine the number of neurons in the hidden layer, which are described as follows.

Among them, the most commonly used method is Trial & Error [71] method. It is considered that an almost optimum number of the hidden layer can be determined using this method. The procedure of this method is explained as follows. First, we set the number of neurons in the hidden layer at a small number, then we start the learning and see the learning results. Basically, we do not get an optimal solution with a single shot, so we will increase the number of neurons in the hidden layer little by little and see the learning results. If the error decreases, we will increase the number of neurons in the hidden layer again. Conversely, if the error increases, we should reduce the number of neurons in the hidden layer. If this procedure is repeated many times and the learning error does not become smaller, we will stop learning and set the number at that time to the number of neurons in the hidden layer.

Determination of the learning times is also important for learning of neural networks. In this study, we decided to start learning after setting learning times. As the way we decide the number of neurons in the hidden layer, we adjust the learning times while seeing the learning result. If the error is large, we increase the learning times. Otherwise, we reduce the learning times. Also, we decide the degree of weight correction and gain in the same way. The gain is a parameter in the sigmoid function.

We assume that the inputs are (x_0, x_1, \dots, x_L) , and the outputs are (y_0, y_1, \dots, y_L) , the learning procedure of the backpropagation method could be expressed as Fig. 4.4.1. We can see that the learning process is the same as we described before. First, set random initial values for the parameters. In this research, the parameters mean the weights of each neuron. Then, prepare the training data which are used to determine the parameters. After providing the inputs to the neural network, the outputs of each neuron in each layer will be calculated so that we could obtain the actual output. Then, the program will execute the backward mode for modifying the values of the weights.

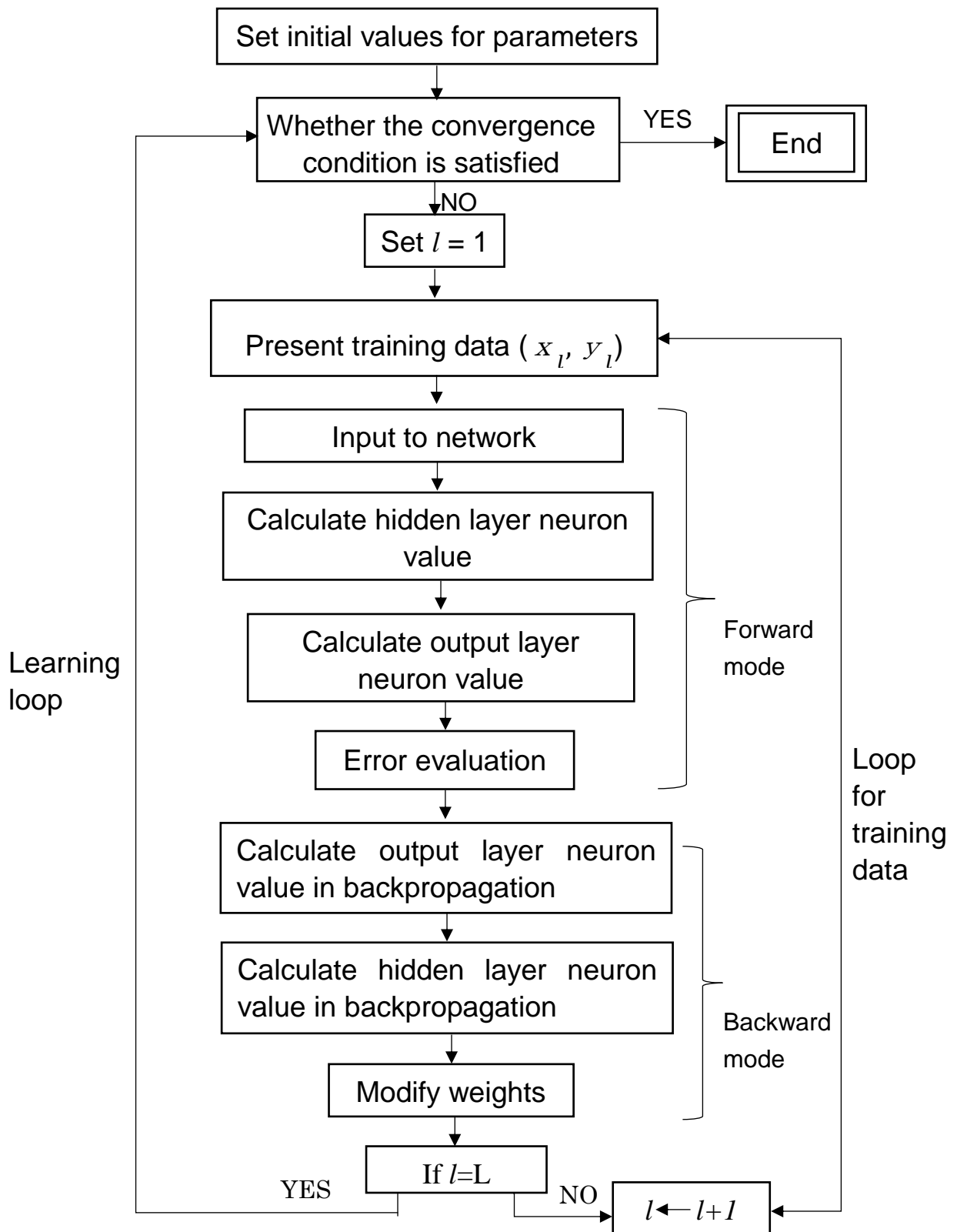


Fig.4.4.1. Learning procedure of the backpropagation method.

5. Experiments and Results

5.1 Experiment for Investigating the Characteristics of an FBG and Results

As described in previous section, we developed a small-size, low cost FBG strain sensor system. The sensor system uses a narrowband light source and a power meter. We calculate the amount of strain applied to the FBG by measuring the reflected power of the FBG. All the experiment are conducted based on this measurement principle.

First, we did the experiment for investigating the strain characteristics of a FBG sensor using one single FBG based on the measurement principle describes in previous section. In the experiment, we measured the change in the reflected power of the FBG using a laser diode light source and a power meter. Then the amount of strain is calculated using the actually measured reflected power. The experiment was performed using the experimental setup shown in Fig. 5.1.1 [36].

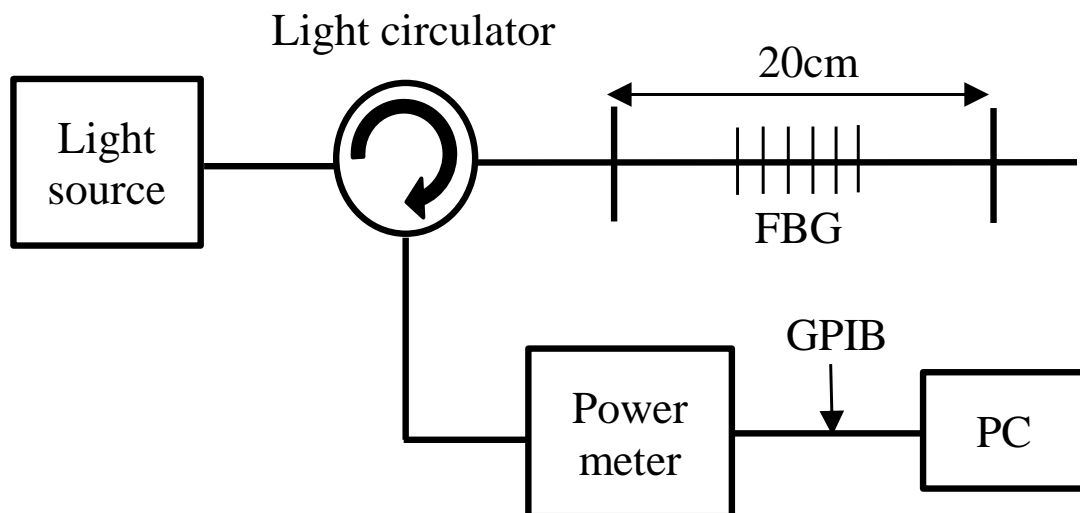


Fig. 5.1.1. Schematic diagram of experimental setup.

The center wavelength of the light source used here is 1549.2 nm, the Full-Width Half-Maximum (FWHM) is 0.203 nm, and the power 30 μ W. The center wavelength of the FBG with 10-mm-long grating used in experiment is 1545.043

nm, the FWHM is 0.552 nm, and the reflectivity is 11.90%.

In the experiment, we fixed the FBG using two magnet stands 20 cm apart. And, we applied strains to the FBG by straining the FBG using a micrometer screw for every 0.01mm. As described in the previous section in which the measurement principle was introduced, when the FBG is strained, the reflectivity of the FBG changes, resulting in a change in the reflected power from the FBG. That is why the strains applied to the FBG can be obtained from the reflected power of the FBG. When the light emitted from the narrow-band light source is incident on the FBG, the reflected power from the FBG will be displayed on the power meter after it is taken out by the optical circulator. Then we store the measured reflected power into a personal computer (PC) connected to a general-purpose interface bus (GPIB). The strain experiment described here is conducted at the same temperature to avoid the effect of temperature changes.

The reflected power depends on the difference between the laser wavelength and the center wavelength of the FBG. Before the experiment, we should adjust the center wavelength of the FBG to the point where it is slightly past the peak as an initial tension. There are two purposes why we have to do the adjustment. One is to ensure that the reflected power changes monotonically, and the other one is to obtain the maximum reflected power at the same time. When strains are applied to the FBG, the measured reflected power will change. The change in reflected power is shown in Fig. 5.1.2 [36] when the FBG is strained. From Fig. 5.1.2, we can observe that the reflected power of the FBG becomes smaller and smaller as the amount of strains applied to the FBG increases. In addition, when the amount of strain changes from 150 to 800 $\mu\epsilon$, the reflected power is

monotonically changing. Thus, we can get a unique and determined strain for a determined reflected power value. Therefore, we also use this interval as a measurement range and performed the function fitting at this monotonic interval. We can obtain an approximate expression of the amount of strain represented by the reflected power through the function fitting. The function fitting is shown in Fig. 5.1.3 [36].

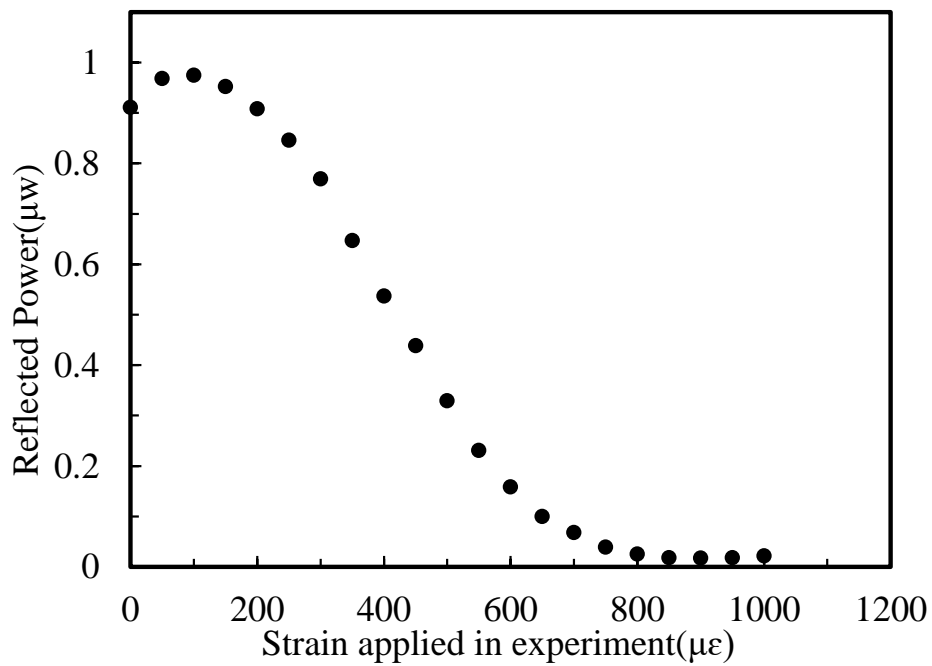


Fig. 5.1.2. Relationship between reflected power and amount of strain applied in the experiment.

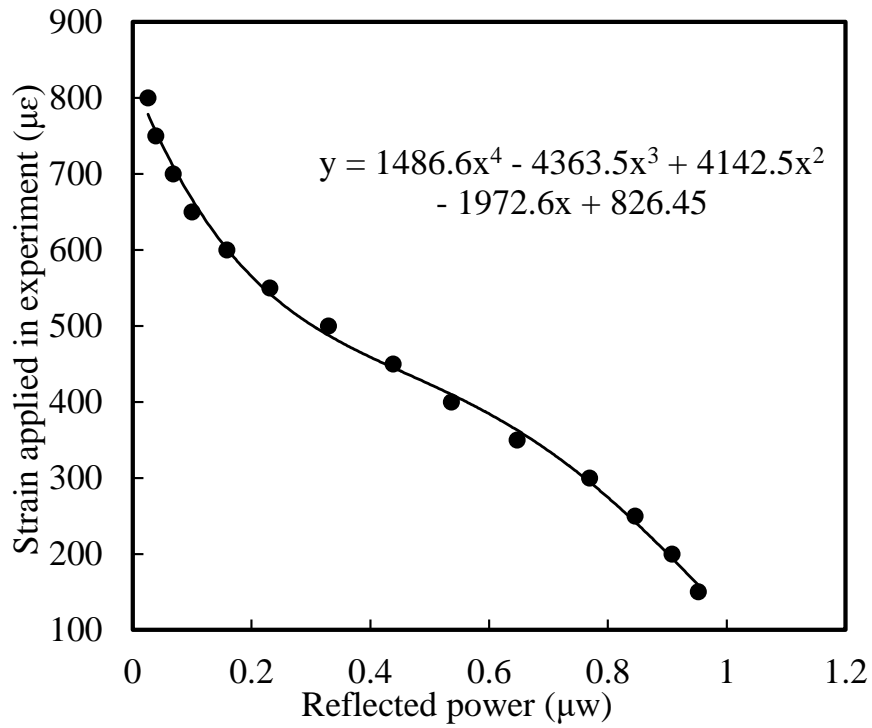


Fig. 5.1.3. Function fitting.

Here, the amount of strain ε can be expressed by the percentage ratio between the elongation Δd of the FBG and the fixed interval d (20cm) of the FBG, given by [36]

$$\varepsilon = \frac{\Delta d}{d} \times 100\%. \quad (5.1.1)$$

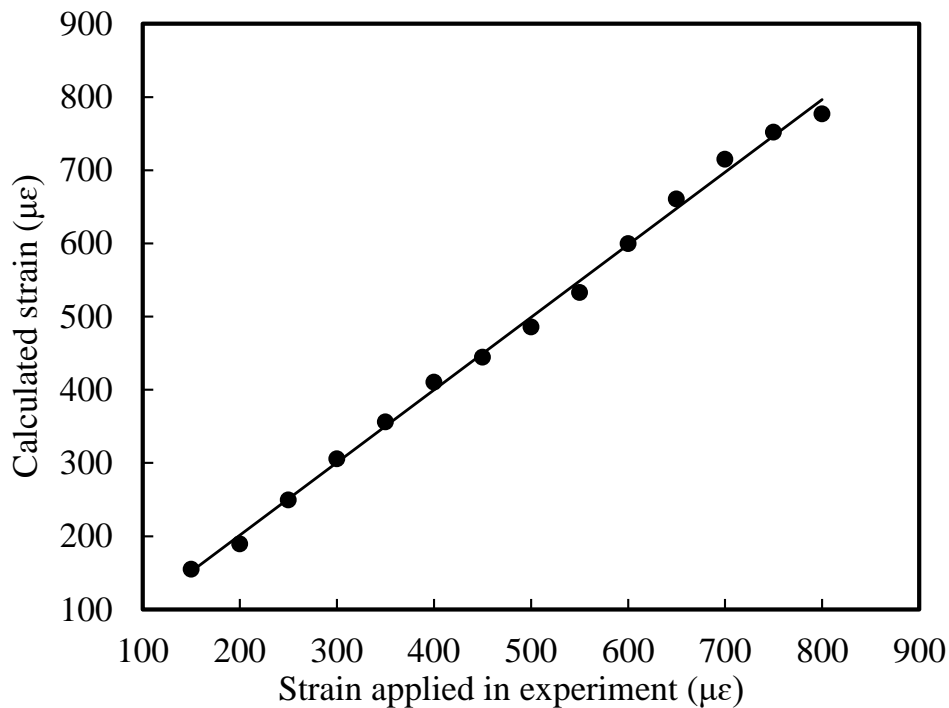


Fig. 5.1.4. Comparison of calculated strain with strain applied in the experiment.

We substituted a newly measured reflected power into the approximate equation shown in Fig. 5.1.3 to calculate the strains. Then, the calculated strains were compared with the strains actually applied in the experiment, and the comparison between them is shown in Fig. 5.1.4 [36]. We can find that there is an approximately linear relationship between the calculated strains and the strains applied in the experiment from Fig. 5.1.4. We can say that they in agreement with each other. In addition, we calculated the relative errors between the actually applied strains and the calculated strains, as shown in Table 5.1.1 [36].

Table 5.1.1. Relative errors between applied and calculated strains using function fitting.

Strain applied in experiment ($\mu\epsilon$)	Calculated strain ($\mu\epsilon$)	Relative errors (%)
150	155.1	3.4
200	189.7	5.1
250	249.5	0.2
300	305.9	2.0
350	356.4	1.8
400	410.5	2.6
450	444.8	1.1
500	486.2	2.8
550	533.4	3.0
600	599.9	0.0
650	660.8	1.7
700	715.4	2.2
750	752.3	0.3
800	777.3	2.8

We can observe that the relative errors are within 5.1% by comparing the strain applied in the experiment with the calculated strain. This means that we can use the calculated strain to replace the actually applied strain. This also indicates that the strain measurement method developed in this research is feasible. At the same time, as mentioned earlier, the strain measurement range of the FBG sensor is found to be 650 $\mu\epsilon$ considering the error. Since we applied strains manually throughout the experiment, this is considered to be one cause of the errors. In addition, it is also considered to reduce errors by improving the accuracy of the function fitting. However, the accuracy improvement is limited. Moreover, the calculations will become very complicated when the number of

FBG increases. Therefore, we propose to use neural networks for data processing to determine the relationship between reflected power and strains of the FBG. In this way, even if the number of FBG increases, we only need to change the inputs and outputs of the neural network and perform appropriate parameter settings to get the desired results.

5.2 Results of the Characteristics Investigating Experiment using a Neural Network

As described in the previous section, any function can be approximated with high precision using a feedforward neural network composed of three layers of an input layer, a hidden layer, and an output layer. Therefore, we decided to use a three-layer feedforward neural network to obtain the relationship between the reflected power of the FBG and the strains applied to the FBG. In the study, the strains applied to the FBG are the values that we expected, so we use the amount of the strain as the output, and the measured reflected power of the FBG is used as the input. That is, the experimental data is provided to the neural network as training data for determining the weights of the neurons, and the relationship between the inputs and outputs is obtained through appropriate learning. Since there is only one single FBG used in this experiment for investigating the strain characteristics of an FBG sensor, correspondingly, there is only one input and one output in the network when using a feedforward neural network for data processing. The feedforward neural network we used is shown in Fig. 5.2.1. There is only one hidden layer. All the parameters used to execute the C program are as follows:

Number of neurons in the hidden layer: 3

Number of learning times: 300000 times

Degree of weight correction ρ : 0.35

Gain α : 1.9

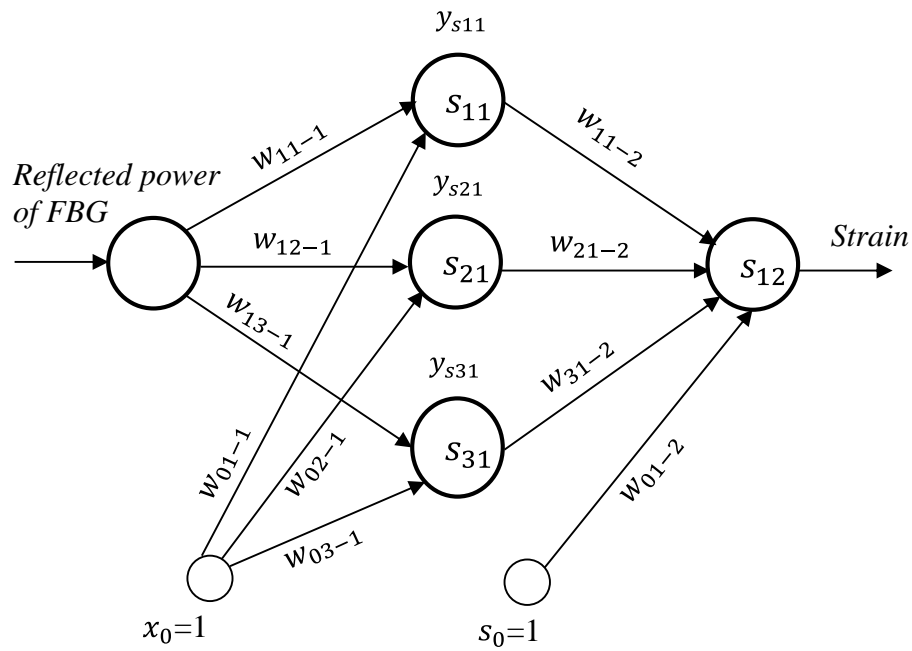


Fig. 5.2.1. Neural network for one FBG.

Table 5.2.1. Different attempts to determine the parameters.

Learning times ($\times 10^4$)	Error evaluation	Learning time (sec)
30	0.000239	31.2
60	0.000224	57.6
100	0.000215	95.6
200	0.000209	160.2

The values for the parameters are not arbitrarily determined. We described how

we should set the parameter values in Chapter 4 where we give the descriptions of the neural network design. As shown in Table 5.2.1, we have made a lot of attempts to determine the values of these parameters before we determined the values.

From Table 5.2.1, we can observe that increasing the number of learning times will reduce the error, but it also increases the learning time. Therefore, when setting parameter values, it is not possible to consider only one but to consider all the parameters comprehensively. It requires both high accuracy and appropriate learning time. Therefore, considering various aspects comprehensively, we determined the values of the above parameters. We also tried with different numbers when determining the number of neurons in the hidden layer. We decided to use three neurons in the hidden layer because even if we increased the numbers, the accuracy did not change.

By executing the C program for learning using the designed neural network, we got the output of the neural network for strains. Table 5.2.2 shows the comparison of strains applied to the FBG in the experiment (target output) and strains outputted by the designed neural network. We can see that the error between the output of the neural network and the values applied in the experiment are very small. As we can see from comparing Table 5.1.1 with Table 5.2.2, the accuracy is promoted using neural network than using the function fitting. In addition, Figure 5.2.2 shows the relationship between the strain applied to the FBG and the reflected power of the FBG. The blue dots represent the experimental data, while the red dots represent the learning results of the neural network. As we can see from the figure, the two sets of data almost coincide,

which also proves that learning has been carried out correctly.

Table 5.2.2. Relative errors between applied and calculated strains using a neural network.

Applied strain in experiment ($\mu\epsilon$)	Output of network ($\mu\epsilon$)	Error (%)
150	147.6	1.6
200	191.5	4.2
250	258.2	3.3
300	307.5	2.5
350	347.6	0.7
400	401.0	0.2
450	446.2	0.9
500	500.2	0.0
550	545.8	0.8
600	595.0	0.8
650	644.9	0.8
700	740.7	0.7
750	754.5	0.6
800	791.0	1.1

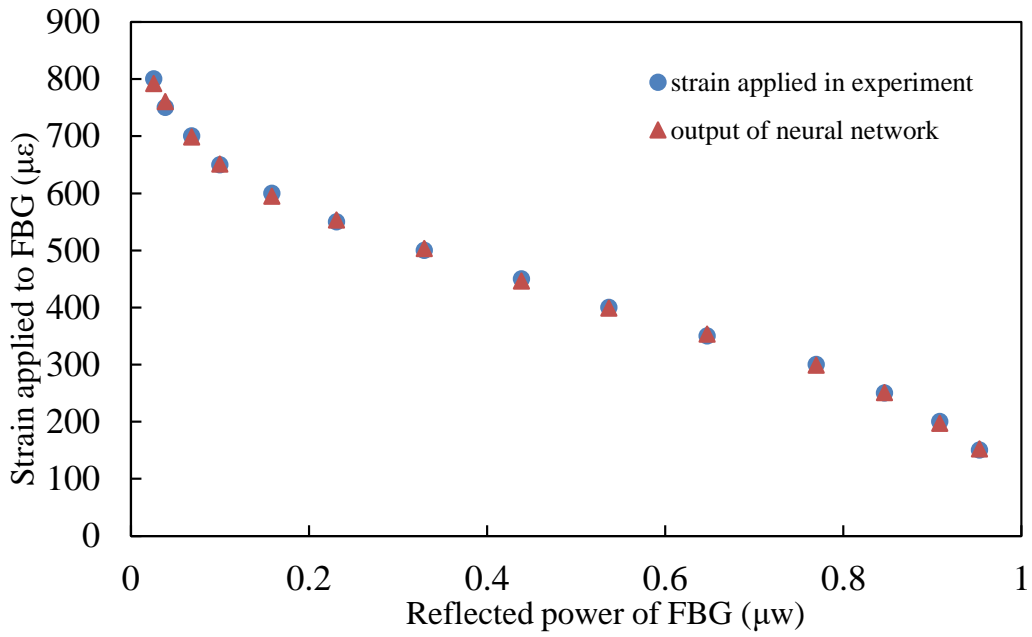


Fig.5.2.2. Comparison of strain applied to the FBG in the experiment (target output) and strain output by the neural network.

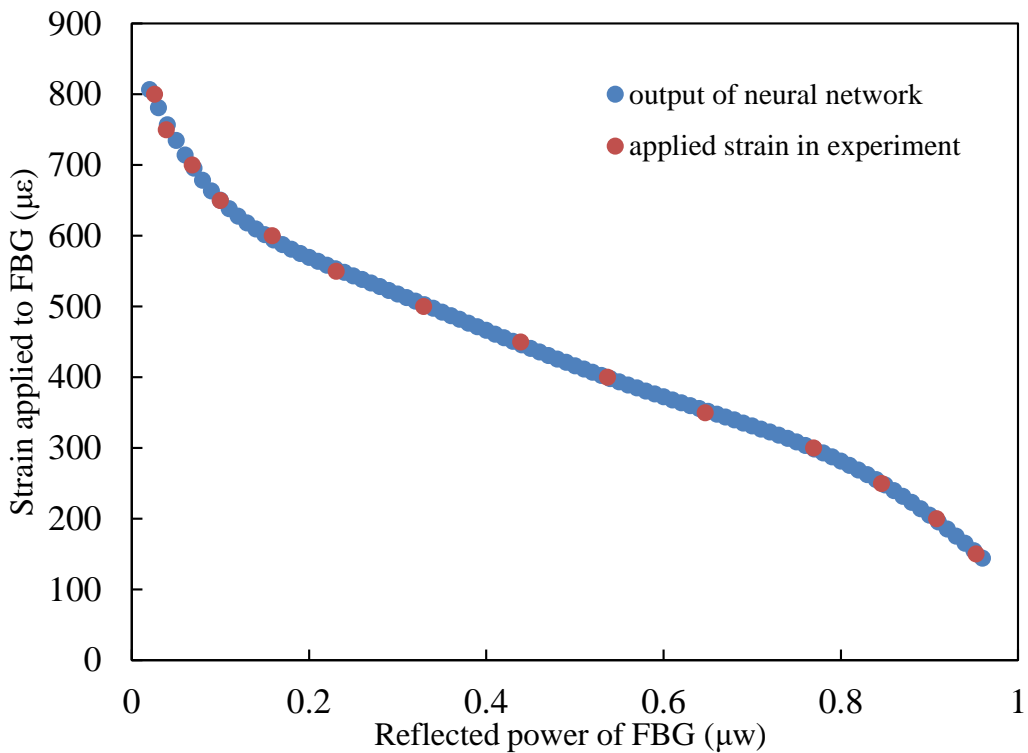


Fig.5.2.3. Comparison of strain applied to the FBG in experiment (target output) and output of the neural network for data other than training data.

As explained in Chapter 4, the target function is approximated by modifying the values of the weights when performing the learning. Therefore, it is possible to calculate the output for data other than the training data using the modified weights.

From the experimental results, we know that the reflected power of the FBG is monotonically changing with the increase of the strain applied to the FBG. Therefore, we can change the value of the reflected power with constant increments within the change range of the reflected power to obtain a set of reflected power values. Then we take this set of reflected power values as inputs to the network and use the modified weight values to calculate the corresponding outputs. The results calculated for this set of reflected power values are shown in Fig. 5.2.3. The red dots represent the relationship between the strains applied in the experiment and the measured reflected power which are used as the training data, while the blue dots represents the relationship between the reflected power other than the training data and the strains outputted by the neural network. We can see that they are all on the same curve, which means the learning for the data other than the training data is correct.

5.3 Temperature Compensation Experiment and Results

As we all know, the FBG is not only sensitive to external strains but also sensitive to changes in temperatures. Therefore, FBGs are not only widely studied as a strain sensor, there is also much research for measuring temperature using FBGs. Because of the sensitivity to temperature, temperature compensation is a difficult point when measuring strains. In order to be able to remove the effects of temperature changes and accurately measure strains, we

must do temperature compensation experiments.

In this study, we performed the experiment using a series of two connected FBGs based on the measurement principle described in Chapter 3. The experimental setup is shown in Fig. 5.3.1. The method for fixing both FBGs is the same as in the FBG strain characteristic investigation experiment. In order to observe the reflected light of multiple FBGs, we used an oscilloscope as a measurement instrument in this experiment. This still makes the experimental system remain miniaturized. We call the former one FBG1 and the latter one FBG2. We used the FBG1 as a temperature measurement sensor to detect the temperature conditions of both FBGs and used the FBG2 as a strain sensor. As can be seen from the experimental setup shown in Fig. 5.3.1, since FBG1 and FBG2 are in the same thermostat, the temperature applied to the two FBGs is also the same. However, the measurement will become difficult if the reflected spectrum of the two FBGs overlaps. Therefore, we used long enough extra optic fiber to connect the two FBGs preventing overlap of reflected spectrum of the two FBGs. The length of the fiber is calculated using the calculation method introduced in Chapter 3.

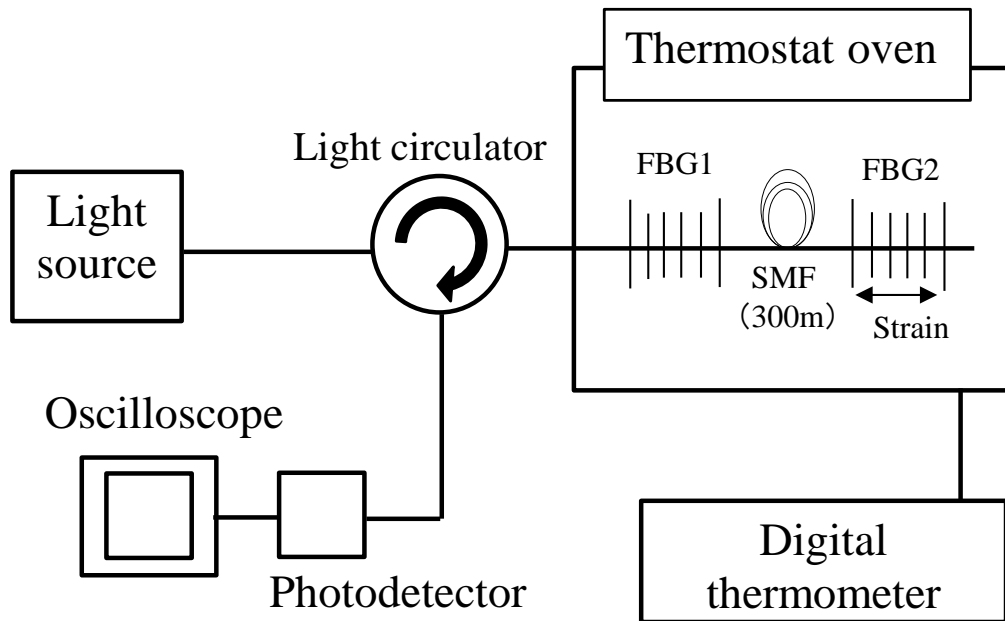


Fig. 5.3.1. Experimental setup using two FBGs connected in series.

In the experiment, we use a thermostat to heat both FBGs simultaneously to ensure that the two FBGs are at the same temperature. We apply strains to FBG2 by stretching FBG2 using a micrometer screw. The reflected light of the two FBGs is measured by an oscilloscope. When the two FBGs are heated, the reflected light of FBG1 changes with the change in temperature. In this way, we can get the relationship between temperature and reflected light of FBG1. Then we can obtain the approximate expression of the temperature of FBG1 represented by the reflected light of the FBG1 by performing a function fitting. In this way, we could calculate the temperature for both FBGs using the reflected power of FBG1. The temperature of FBG1 is also that of FBG2. In the same way, we can also obtain an equation of the strains of FBG2 expressed by the temperature and the reflected light of FBG2. Then by substituting the temperature of the FBGs and the reflected light of FBG2 into the equation of the strain of FBG2, we can determine

the strain of FBG2 even when the temperature changes. The change in the reflected power of FBG1 is shown in Fig. 5.3.2 when the FBGs were heated. In the experiment, the temperature was changed from 24°C to 44 °C for every 1 °C, and strains was applied to FBG2 from 0 to 450 $\mu\epsilon$ for every 50 $\mu\epsilon$.

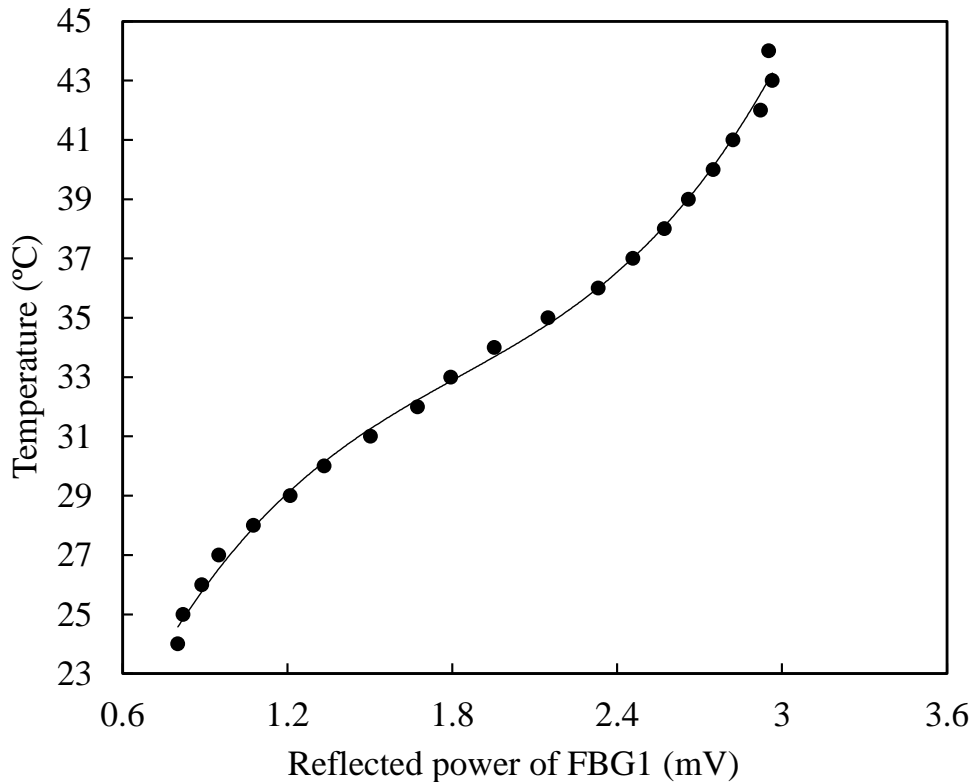


Fig. 5.3.2. Temperature versus reflected power of FBG1.

From Fig. 5.3.2 we can see that the reflected power changes monotonically when the temperature changes. Then, we could give an approximate expression of the temperature expressed by the reflected power of FBG1 by performing function fitting. Then, we could use the approximate expression to calculate the temperature of FBG1, which is also the temperature of FBG2. The relationship between the reflected power of FBG2 and the strains applied to FBG2 under different temperatures is shown in Fig. 5.3.3.

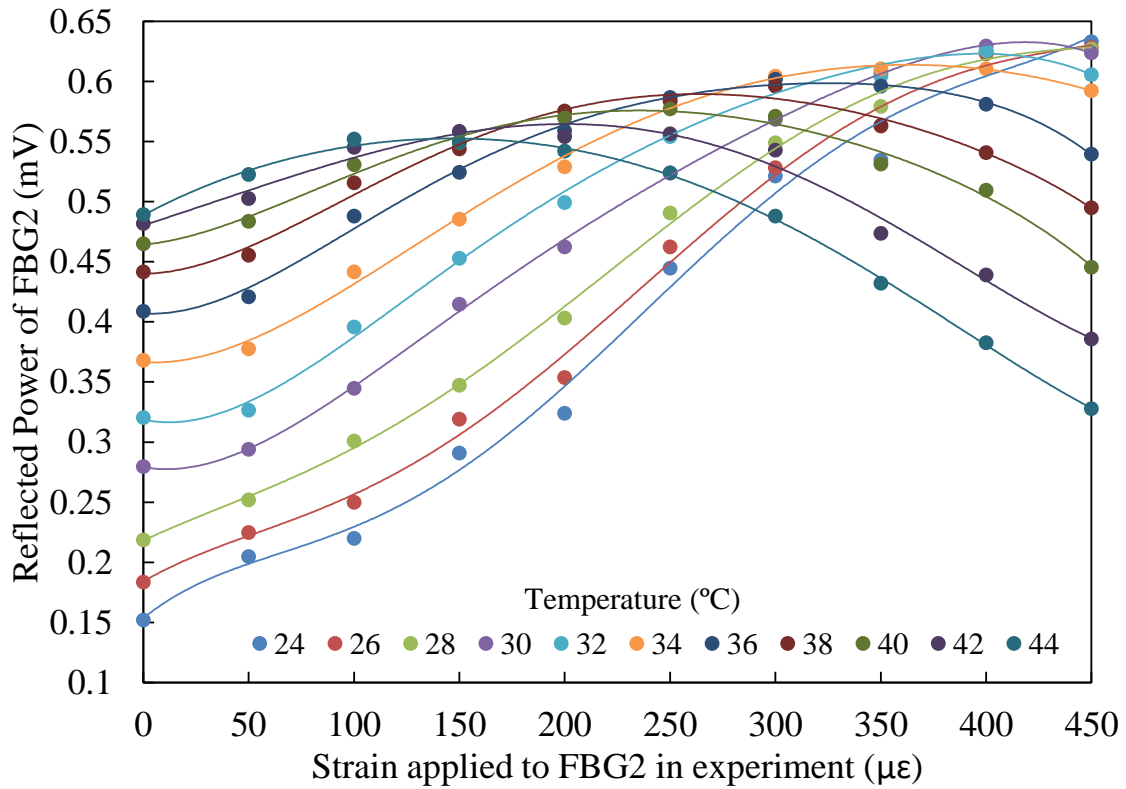


Fig. 5.3.3. Reflected power versus strains of FBG2 under different temperatures.

If we can find the relationship between strains and the reflected light of FBG2 under different temperatures, then we can obtain the strains of FBG2 from the measured reflected light. The 3-dimensional graph of strain, temperature and reflected power of FBG2 is shown in Fig.5.3.4.

From Fig.5.3.4 we can see that the reflected power does not change monotonically with the change in strain when the temperature remains constant. When the reflected power is between 0.55 mV and 0.65 mV, we can observe that the curved surface is turning up. In this range, when the temperature remains constant, even if the strain is different, the reflected power can be the same. This is because the reflectivity of an FBG is symmetrical and we can learn that from the measurement principle described in Chapter 3. This leads to the situation that the strain cannot be correctly calculated. Therefore, the measurement range

should be limited to the range before the curved surface turns up to ensure that when the temperature remains the same, the reflected power of FBG2 will change monotonically with the changes in strains. Taking this and the error into account, we determined the measurement range in which the temperature changed from 27 °C to 37 °C and the strain was from 100 $\mu\epsilon$ to 300 $\mu\epsilon$.

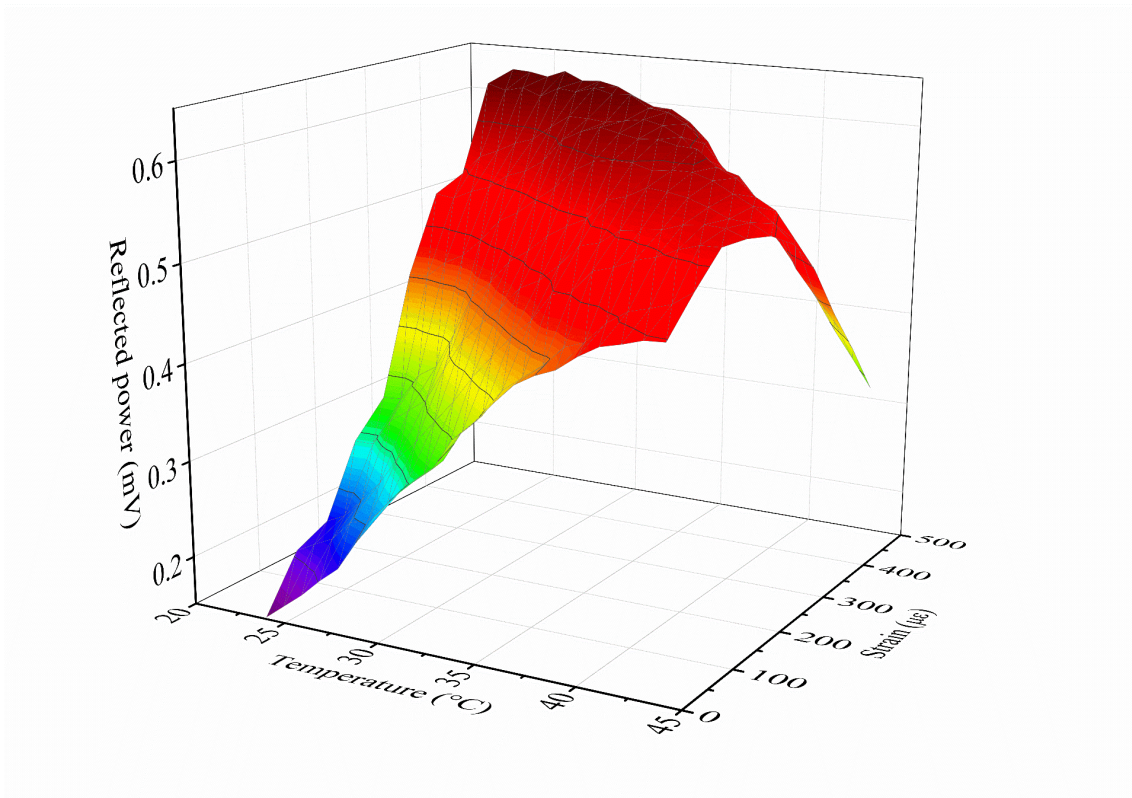


Fig. 5.3.4. 3-dimensional graph of FBG2's measurement results.

Then, we performed a curved surface fitting in the limited range and got a curved surface equation with an R-square of 0.9833. Substituting the temperature and the strains of FBG2 into the curved surface equation, we determined the calculated strains of FBG2. The comparison of FBG2's calculated strains and strains applied in the experiment with temperature compensation is shown in Fig. 5.3.5. To illustrate the importance of temperature compensation, we also gave results without temperature compensation, and the comparison of FBG2

calculated strains and strains applied in the experiment without temperature compensation is shown in Fig. 5.3.6.

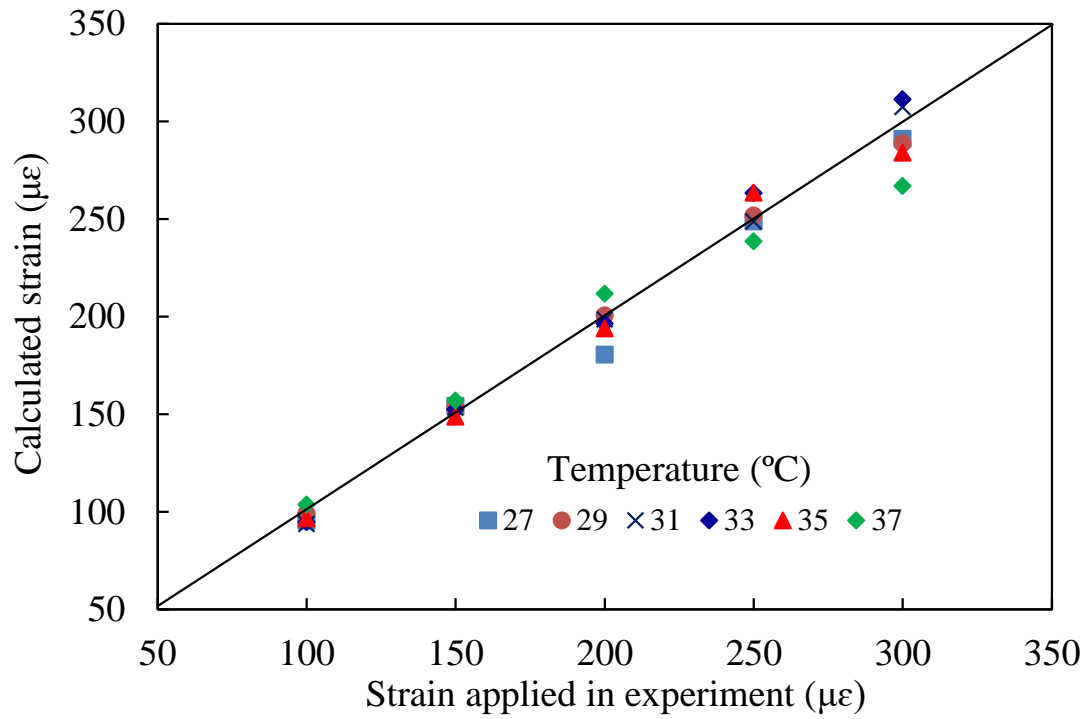


Fig. 5.3.5. Comparison of FBG2's calculated strain and strain applied in the experiment with temperature compensation.

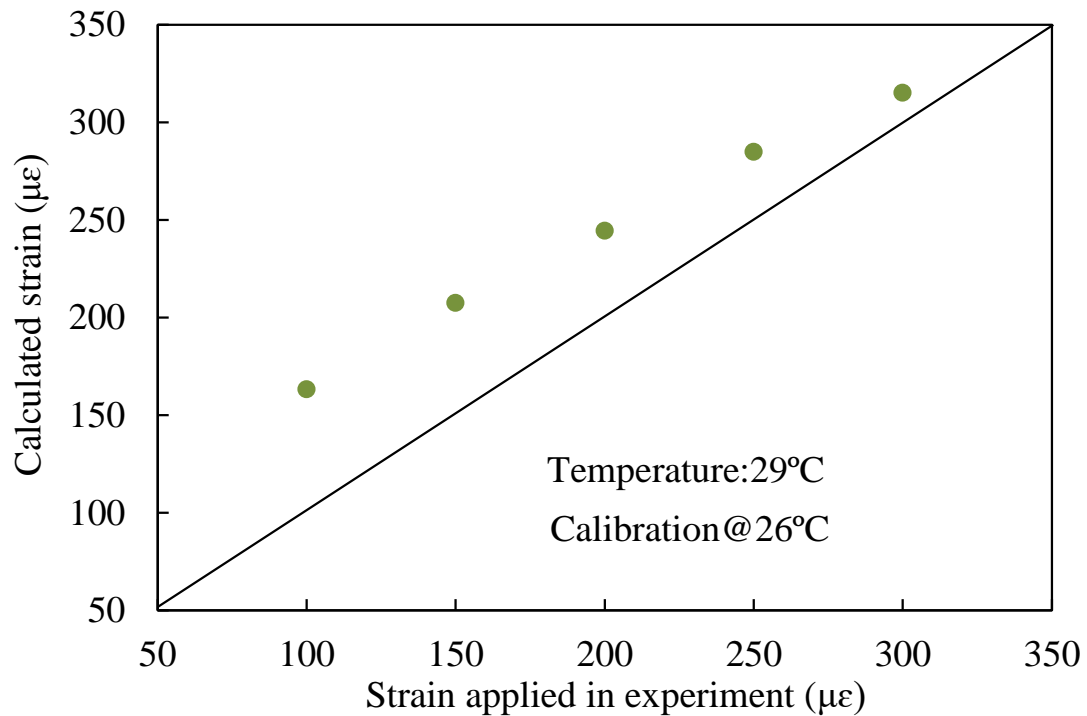


Fig. 5.3.6. Comparison of FBG2's calculated strain and strain applied in the experiment with temperature compensation.

Compare Fig. 5.3.5 with Fig. 5.3.6, we can find that when not compensating for temperature, considerable errors appeared between the calculated strains and the strains applied in the experiment although the temperature changes only by 3 °C. The accuracy was pretty improved through temperature compensation. In addition, due to the complexity and difficulty of surface fitting and the limited accuracy, large errors appeared between the strains calculated using the fitting function and the strains actually applied in the experiment. When introducing the problem of measuring the temperature at multiple points, we also mentioned that when the number of FBGs increases, the function fitting will become very difficult, and the error will further increase. Therefore, we decided to use a feedforward neural network for data processing to obtain the relationship between strain, temperature, and reflected power of FBG2 with high accuracy.

5.4 Results of Temperature Compensation Experiment by a neural network

In the experiment, there are only two FBGs connected in series, we can give a 3-dimensional graph representing the results of FBG2. However, as the number of FBGs increases, the number of parameters increases and the aforementioned method of function fitting will no longer apply. Therefore, we decided to use a neural network to deal with the function approximate.

As described in Chapter 4, a proper design of the neural network is very important to get desired results. As described in the previous section, any function can be approximated with high precision by a feedforward type neural network composed of three layers of an input layer, a hidden layer, and an output layer. Therefore, we decided to use a three-layer feedforward neural network to obtain the relationship between inputs and outputs. In the study, the temperature of the two FBGs and the strains applied to FBG2 are the values that we expected, so we use the temperature and strains as outputs, and the measured reflected power of both FBGs are used as the inputs. The flow is shown in Fig. 5.4.1. There is only one hidden layer. All the parameters used to execute the C program are as follows:

Number of neurons in the hidden layer: 10

Number of learning times: 2000000 times

Degree of weight correction ρ : 1.0

Gain α : 1.9

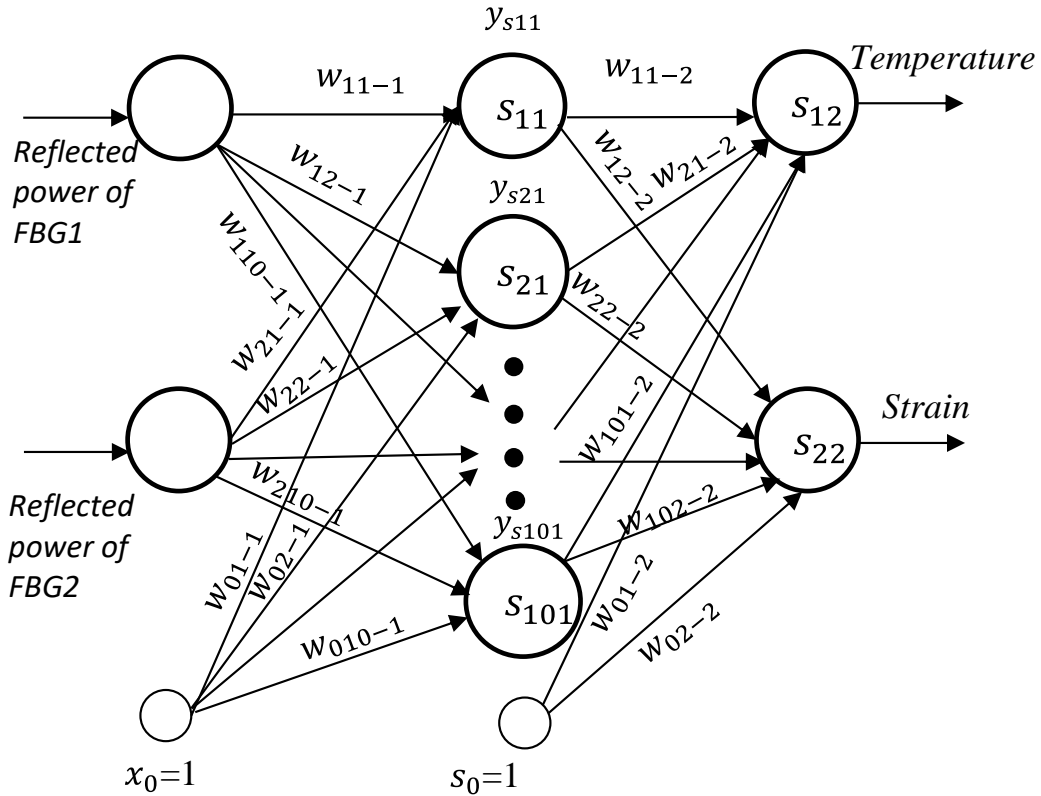


Fig. 5.4.1. Neural network for two FBGs connected in series.

Just as we did in the FBG strain characteristic investigation experiment, we made a lot of attempts for each parameter before we finally decided on these parameter values. By executing the C program for learning using the designed neural network, we got the output of the network for temperatures and strains. Figure 5.4.2 shows the comparison of temperature applied in the experiment (target output) and temperature outputted by the designed neural network. We can see that the output of the designed neural network is almost the same as the values applied in the experiment.

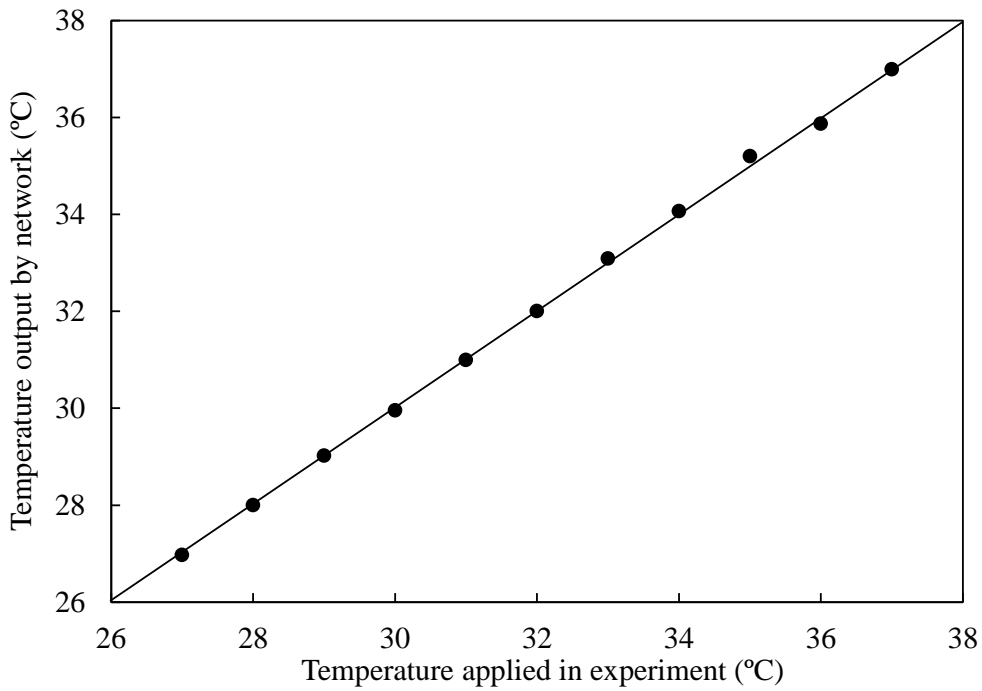


Fig. 5.4.2. Comparison of temperature applied in experiment and temperature output by the neural network.

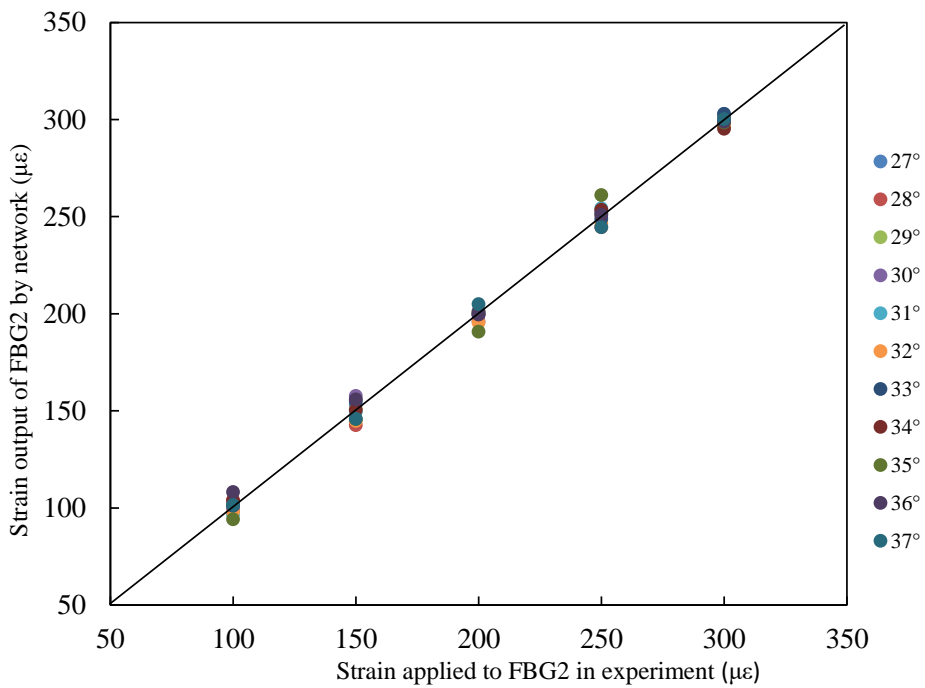


Fig. 5.4.3. Comparison of the strains applied to FBG2 in experiment at each temperature and the output strains by the neural network.

The comparison of the strains applied to FBG2 in the experiment (target output) at each temperature and the outputted strain by the neural network is shown in Fig. 5.4.3. The strains applied in the experiment and the strains outputted by the designed neural network are almost the same. In addition, comparing Fig. 5.3.5 with Fig. 5.4.3, the accuracy was pretty improved using a feedforward neural network to do the data processing.

However, the purpose of learning is to acquire the ability to give correct outputs for inputs other than training data. Within the measurement range, we change the reflected power values with constant increments within the change range of the reflected power at different temperatures and use these power values as inputs to the designed neural network. Then we use the modified weights to calculate the outputs, which are also the strain values corresponding to these powers. The learning results are shown in Fig. 5.4.4 ~ Fig. 5.4.7.

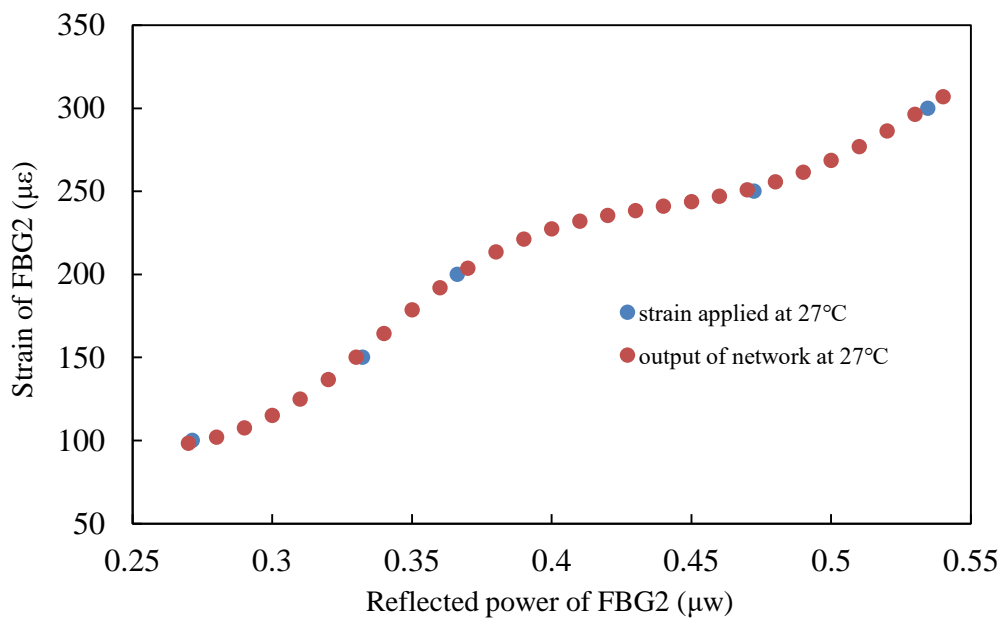


Fig. 5.4.4. Learning results for data other than training data at 27°C.

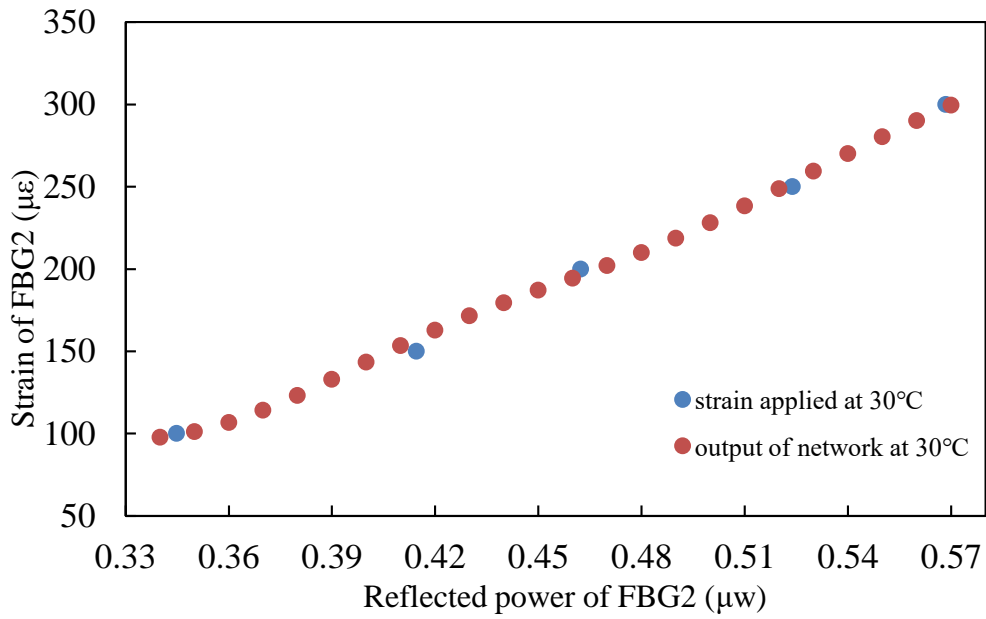


Fig. 5.4.5. Learning results for data other than training data at 30°C.

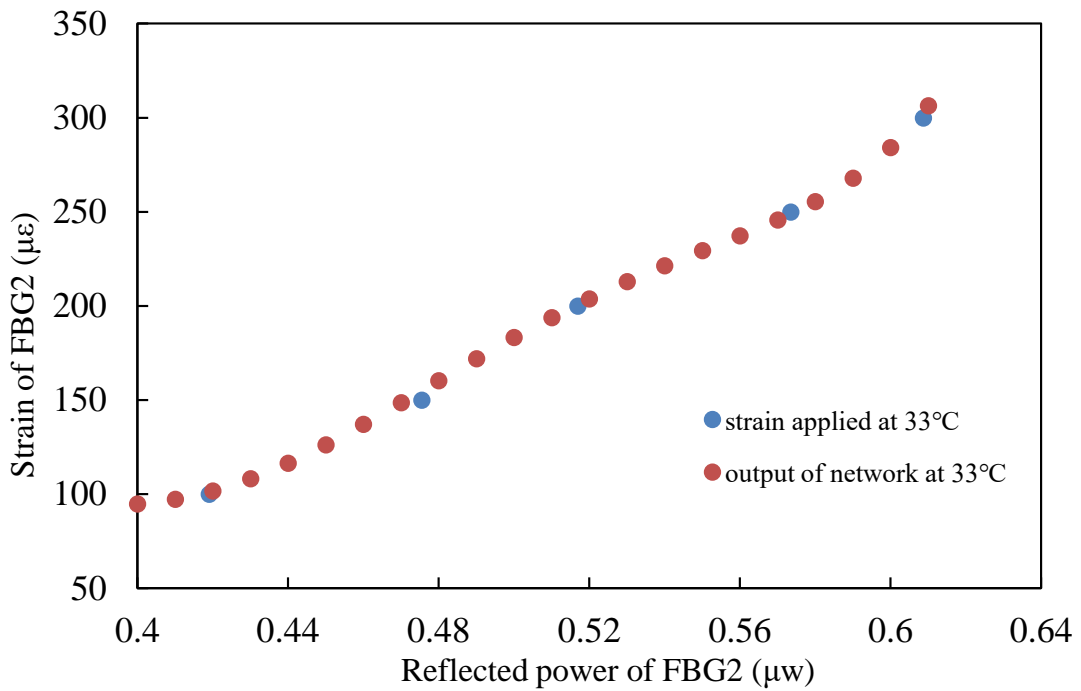


Fig. 5.4.6. Learning results for data other than training data at 33°C.

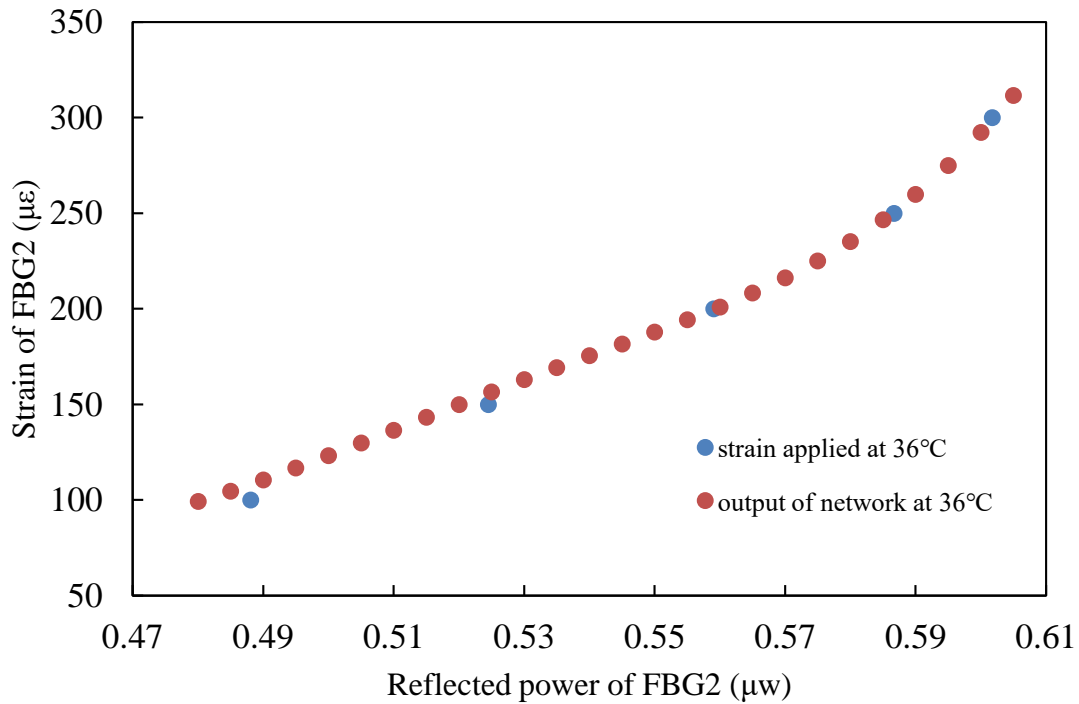


Fig. 5.4.7. Learning results for data other than training data at 36°C.

In these figures, the blue dots are experimental data which are used to determine the weights, while the red dots are the data not used to determine the weights. We can see from the figures that the blue dots and the red dots change in the same way, and they are all on the same curve. With these results, we were able to obtain the correct outputs for inputs other than training data. Moreover, with these results, we can say that we not only performed the learning correctly but also calculated the outputs for the data other than training data. Thus, although in experiments, we could not continuously measure the changes in reflected power to determine the strains applied to the FBG. But through this method, we could find the relationship between strains and reflected powers at different temperatures. In this way, as long as the strain changes within the measurement range of the sensor system, we can find the corresponding strain

values for any one of the reflected power values. And this strain value is the value after the influence of temperature is removed, which also means the temperature compensation is successfully performed.

6. Conclusions

6. Conclusions

FBG sensors are widely researched and used to measure strains, temperatures, pressures, and vibrations. Since conventional FBG strain sensors analyze reflection spectrum and measure the shift in reflected wavelength due to strain changes, a broadband light source and an optical spectrum analyzer are indispensable devices, which make the measurement system large and expensive. In view of this, in this study, we proposed a strain sensor system for measuring strains from the reflected power of FBGs. In the sensor system, we use a laser diode as the light source and use a power meter as the measurement device. This makes the FBG strain sensor system small-size and less costly than the conventional FBG sensor system. In addition, we gave descriptions of FBGs, measurement principles, and neural networks used to process data. Based on the FBG strain measurement method proposed in the study, we can perform multipoint measurement by using the time delay of reflected pulses of multiple FBGs connected in series. Based on the principle of multipoint measurement, we used two FBGs connected in series to conduct the temperature compensation experiment. Moreover, we used a feedforward neural network with a powerful function approximation to find the relationship between strains, temperatures, and the reflected power.

In this study, the experiment was divided into two parts. First, we conducted the FBG strain characteristic investigation experiment using a single FBG based on the proposed strain measurement method. To avoid the effects of temperature changes, we performed the experiment at the same temperature. In order to find out the relationship between the strains and the reflected power of the FBG, we

used function fitting and neural network to find the relationship between strains and reflected power, respectively. The strains calculated by these two methods were compared with the strains applied to the FBG in the experiment. We have come to the conclusion that the results calculated by the neural network have smaller errors and higher accuracy.

Second, we did the temperature compensation experiment using two series-connected FBGs. And, we compared the calculated strains with temperature compensation and that without temperature compensation. We can know that the accuracy was pretty improved with temperature compensation from the comparison. This also explains the importance and necessity of temperature compensation in FBG strain experiment. The experimental results also prove the effectiveness of the temperature compensation method.

In the temperature compensation experiment, we also used function fitting and neural network separately to find the relationship of the temperatures, strains, and the reflected power. The strains calculated by the two methods are compared with each other. The results obtained by the neural network are much better than those obtained by the function fitting. In addition, in both experiments, we obtained the corresponding strains for the reflected power other than the measured reflected power. Therefore, we can say that the feasibility of the proposed strain sensor system has been verified by experimental results. Moreover, based on the proposed measurement method, and using the function approximation function of the neural network to find the relationship of temperatures, strains, and reflected power, it is considered that a multipoint strain measurement with temperature compensation can be realized.

Acknowledgments

My deepest gratitude goes first and foremost to my supervisor, Associate Professor Shinya Sato. It is his invaluable guidance, support and constant encouragement that enable me to finish this dissertation. Secondly, I would like to thank Professor Akira Sakai for his guidance during the weekly meetings and support in the research. And, I would also like to express my thanks to Professor Shigeki Miyanaga for his support in the research and advice in the presentation. I would also like to thank everyone in the laboratory for their support in the research. Thirdly, I would like to express my sincerest thanks to my friends. This dissertation would not be possible without their encouragement and support. Finally, I would like to express my deepest gratitude to my beloved family for their loving considerations and great support over the years. This dissertation is dedicated to them all.

References

1. T. Nagayama, M. Ruiz-Sandoval, B. F. Spencer Jr, K. A. Mechitov, and G. Agha, "Wireless strain sensor development for civil infrastructure", *Trans. of the Society of Instrument and Control Engineers*, vol. E-3, no. 1, pp.104-109 (2004).
2. A. Kalamkarov, G. Saha, S. Rokkam, J. Newhook, and A. Georgiades, "Strain and deformation monitoring in infrastructure using embedded smart FRP reinforcements", *Composites Part B: Engineering*, vol. 36, no. 5, pp.455-467 (2005).
3. R. Srinivasan, and A. K. Parlikad, "Value of condition monitoring in infrastructure maintenance", *Computers & Industrial Engineering*, vol. 66, no. 2, pp. 233-241 (2013).
4. G. Xu, D. Xiong, Y. Duan, and X. Cao, *Optical Engineering*, vol. 54, no.1, pp.011003 (2015).
5. M. Ohn, S. Sandgren, S. Huang, R. Maaskant, R. Stubbe, B. Sahlgren, R. Measures, and H. Storoy, "Phase Based Bragg Intra-Grating Sensing of Strain Gradients", *Proc. SPIE*, vol. 2444, pp. 127-135 (1995).
6. B. Lee, "Review of the present status of optical fiber sensors", *Optical Fiber Technology*, vol. 9, no.2, pp.57-59 (2003).
7. K. Peters, "Polymer optical fiber sensors-a review", *Smart Materials and Structures*, vol.20, no.1, (2010).
8. V. Bhatia, and A. M. Vengsarkar, "Optical fiber long-period grating sensors", *Optics Letters*, vol.21, no.9, pp.692-694 (1996).
9. C. Li, and T. Yoshino, "Optical voltage sensor based on electrooptic crystal

- multiplier”, *Journal of Lightwave Technology*, vol.20, no.5, pp.843-849 (2002).
10. T. G. Giallorenzi, J. A. Bucaro, A. Dandridge, G. H. Sigel, J. H. Cole, S.C. Rashleigh, and R.G. Priest, “Optical fiber sensor technology”, *IEEE Transactions on Microwave Theory and Techniques*, vol.30, no.4, pp.472-511 (1982).
 11. H.N. Li, D.S. Li, and G.B. Song, “Recent applications of fiber optic sensors to health monitoring in civil engineering”, *Engineering Structures*, vol.26, no.11, pp.1647-1657 (2004).
 12. S. Villalba, and J.R. Casas, “Application of optical fiber distributed sensing to health monitoring of concrete structures”, *Mechanical Systems and Signal Processing*, vol.39, pp.441-451 (2013).
 13. D. Luo, Y. Yue, P. Li, J. Ma, L. Zhang, Z. Ibrahim, and Z. Ismail, “Concrete beam crack detection using tapered polymer optical fiber sensors”, *Measurement*, vol.88, pp.96-103 (2016).
 14. J. Zhao, T. Bao, and U. Amjad, “Optical fiber sensing of small cracks in isotropic homogeneous materials”, *Sensors and Actuators A: Physical*, vol. 225, pp.133-138 (2015).
 15. R. Unzu, J.A. Nazabal, G. Vargas, R.J. Hernandez, C.Fernandea-Valdivielso, N. Urriza, M. Galarza, and M. Lopez-Amo, “Fiber optic and KNX sensors network for remote monitoring a new building cladding system”, *Automation in Construction*, vol.30, pp.9-14 (2013).
 16. C. Yang, and S.O. Oyadiji, “Development of two-layer multiple transmitter fibre optic bundle displacement sensor and application in structural health monitoring”, *Sensors and Actuators A: Physical*, vol.244, pp.1-14 (2016).
 17. K. Lau, C. Chan, L. Zhou, and W. Jin, “Strain monitoring in composite-

- strengthened concrete structures using optical fibre sensors”, *Composites Part B: Engineering*, vol.31, no.1, pp.33-45 (2001).
18. R.C. Jorgenson, and S.S. Yee, “A fiber-optic chemical sensor based on surface plasmon resonance”, *Sensors and Actuators B: Chemical*, vol.12, no.3, pp. 213-220 (1993).
 19. T. Hu, Y. Zhao, and A. Song, “Fiber optic SPR sensor for refractive index and temperature measurement based on MMF-FBG-MMF structure”, *Sensors and Actuators B: Chemical*, vol.237, pp.521-525 (2016).
 20. S.W. James, and R.P. Tatam, “Optical fibre long-period grating sensors: characteristics and application”, *Measurement Science and Technology*, vol.14, no.5, (2003).
 21. K. Bohnert, J. Nehring, and H. Brandle, “Temperature and vibration insensitive fiber-optic current sensor”, *Journal of Lightwave Technology*, vol.20, no.2, pp.267-276 (2002).
 22. X. Shu, L. Zhang, and I. Bennion, “Sensitivity characteristics of long-period fiber grating”, *Journal of Lightwave Technology*, vol.20, no.2, pp.255-266 (2002).
 23. T. Ritari, J. Tuominen, and H. Ludvigsen, “Gas sensing using air-guiding photonic bandgap fibers”, *Optics Express*, vol.12, no.17, pp.4080-4087 (2004).
 24. K. Kyuma, and M. Nunoshita, “Optical fiber sensor « Foundation and application »”, pp.81-94, (1986), [In Japanese].
 25. K. Okoshi, H. Nishihara, K. Okamoto, K. Kyuma, M. Otsu, and K. Hotate, “Optical fiber sensors”, Ohmsha, pp.125-160, (1986), [In Japanese].
 26. R.D. Samte, and F. Bastianini, “Temperature-compensated fibre Bragg

- grating-based sensor with variable sensitivity”, *Optics and Lasers in Engineering*, vol.75, pp.5-9 (2015).
27. W. Du, X.M. Tao, H.Y. Tam, and C.L. Choy, “Fundamentals applications of optical fiber Bragg grating sensors to textile structural composites”, *Composite Structures*, vol.42, no.3, pp.217-229 (1998).
 28. M. Majumder, T.K. Gangopadhyay, A.K. Chakraborty, K. Dasgupta, and D.K. Bhattacharya, “Fiber Bragg gratings in structural health monitoring-Present status and applications”, *Sensors and Actuators A: Physical*, vol.147, no.1, pp.150-164 (2008).
 29. S.J. Mihailov, “Fiber Bragg grating sensors for harsh environments”, *Sensors*, vol.12, pp.1898-1918 (2012).
 30. W.W. Morey, G. Meltz, and W.H. Glenn, “Fiber optic Bragg grating sensors”, *Proceedings of SPIE, Fiber Optic and Laser Sensors VII*, vol. 1169, (1990).
 31. J. Huang, Z. Zhou, D. Zhang, X. Yao, and L. Li, “Online monitoring of wire breaks in prestressed concrete cylinder pipe utilising fibre Bragg grating sensors”, *Measurement*, vol. 79, pp.112-118 (2016).
 32. X.X. Li, W.X. Ren, and K.M. Bi, “FBG force-testing ring for bridge cable force monitoring and temperature compensation”, *Sensors and Actuators A: Physical*, vol. 223, pp.105-113 (2015).
 33. R.D. Sante, and L. Donati, “Strain monitoring with embedded fiber Bragg gratings in advanced composite structures for nautical applications”, *Measurement*, vol.46, no.7, pp.2118-2126 (2013).
 34. T.C. Hsiao, T.S. Hsien, Y.C. Chen, S.C. Huang, and C.C. Chiang, “Metal-coated fiber Bragg grating for dynamic temperature sensor”, *Optik-International Journal for Light and Electron Optics*, vol.127, no.22, pp.10740-

10745 (2016).

35. V. Mishra, M. Lohar, and A. Amphawan, "Improvement in temperature sensitivity of FBG by coating of different materials", *Optik-International Journal for Light and Electron Optics*, vol.127, no.2, pp.825-828 (2016).
36. L. Yuan, Y. Zhao, and S. Sato, "Development of a low-cost and miniaturized fiber Bragg grating strain sensor system", *Japanese Journal of Applied Physics*, vol. 56, pp. 052502 (2017).
37. L. Rodriguez-Cobo, A. Cobo, and J.M. Lopez-Higuera, "Embedded compaction pressure sensor based on fiber Bragg gratings", *Measurement*, vol.68, pp.257-261 (2015).
38. Y. Guo, J. Kong, H. Liu, H. Xiong, G. Li, and L. Qin, "A three-axis force fingertip sensor based on fiber Bragg grating", *Sensors and Actuators A: Physical*, vol. 249, pp.141-148 (2016).
39. S.W. Kim, "Characteristics of strain transfer and the reflected spectrum of a metal-coated fiber Bragg grating sensor", *Optics and Lasers in Engineering*, vol. 96, pp. 83-93 (2017).
40. M. Mieloszyk, and W. Ostachowicz, "An application of Structural Health Monitoring system based on FBG sensors to offshore wind turbine support structure model", *Marine Structures*, vol. 51, pp. 65-86 (2017).
41. W.P. Chen, F.H. Shin, P.J. Tseng, C.H. Shao, and C.C. Chiang, "Application of a packaged fiber Bragg grating sensor to outdoor optical fiber cabinets for environmental monitoring", *IEEE Sensors Journal*, vol. 15, no. 2, pp. 734-741 (2015).
42. L. Xia, R. Cheng, W. Li, and D. Liu, "Identical FBG-based quasi-distributed sensing by monitoring the microwave responses", *IEEE Photonics*

- Technology Letters, vol.2 7, no. 3, pp. 323-325 (2015).
43. P.S. Reddy, R.L.N.S. Prasad, D. Sengupta, P. Kishore, M.S. Shankar, K.S. Narayana, and U.K. Tiwari, "Method for enhancing and controlling temperature sensitivity of fiber Bragg grating sensor based on two bimetallic strips", IEEE Photonics Journal, vol. 4, no. 3, pp. 1035-1041 (2012).
 44. https://en.wikipedia.org/wiki/Optical_fiber
 45. D. Dennis, "Fiber optic test and measurement", Prentice Hall PTR, pp. 6-27 (1998).
 46. K. Hotate, and H. Murayama, "Introduction to optical fiber sensors", Photonic Sensing Consortium for Safety and Security, pp. 35-36 (2012), [In Japanese].
 47. T. Tsuruoka, "Optical fiber communication: supporting information infrastructure in the multimedia era", Hitotsubashi Shoten, pp. 36-45 (1997), [In Japanese].
 48. D. Toomre, and D.J. Manstein, "Lighting up the cell surface with evanescent wave microscopy", Trends in Cell Biology, vol. 11, no. 7, pp.298-303 (2001).
 49. K. Hotate, and H. Murayama, "Introduction to optical fiber sensors", Photonic Sensing Consortium for Safety and Security, pp. 19-20 (2012), [In Japanese].
 50. K. Okoshi, H. Nishihara, K. Okamoto, K. Kyuma, M. Otsu, and K. Hotate, "Optical fiber sensors", Ohmsha, pp.125-200, (1986), [In Japanese].
 51. N.M.P. Pinto, O. Frazao, J.M. Baptista, and J.L. Santos, "Quasi-distributed displacement sensor for structural monitoring using a commercial OTDR", Optics and Lasers in Engineering, vol. 44, no. 8, pp. 771-778 (2006).
 52. D.V. Caballero, R.P. Almeida, P.J. Urban, J.C.W.A. Costa, J.P. von der Weid, and J. Chen, "SCM/WDM-PON with in-service baseband embedded OTDR monitoring", Optics Communications, vol. 356, pp. 250-255 (2015).

53. H. Ohno, H. Naruse, M. Kihara, and A. Shimada, "Industrial applications of the BOTDR optical fiber strain sensor", *Optical Fiber Technology*, vol. 7, no. 1, pp. 45-64 (2001).
54. A. Motil, A. Bergman, and M. Tur, "State of the art of Brillouin fiber-optic distributed sensing", *Optics & Laser Technology*, vol. 78, Part A, pp. 81-103 (2016).
55. R. Moffat, J. Sotomayor, and J.F. Beltran, "Estimating tunnel wall displacements using a simple sensor based on a Brillouin optical time domain reflectometer apparatus", *International Journal of Rock Mechanics and Mining Sciences*, vol. 75, pp.233-243 (2015).
56. Y. Li, C. Wen, Y. Sun, Y. Feng, and H. Zhang, "Capillary encapsulating of fiber Bragg grating and the associated sensing model", *Optics Communications*, vol. 333, pp. 92-98 (2014).
57. J. Dai, M. Yang, X. Li, H. Liu, and X. Tong, "Magnetic field sensor based on magnetic fluid clad etched fiber Bragg grating", *Optical Fiber Technology*, vol. 17, pp. 210-213 (2011).
58. Z. Zhou, W. Liu, Y. Huang, H. Wang, J. He, M. Huang, and J. Ou, "Optical fiber Bragg grating sensor assembly for 2D strain monitoring and its case study in highway pavement", *Mechanical Systems and Signal Processing*, vol. 28, pp. 36-49 (2012).
59. I.C. Song, S.K. Lee, S.H. Jeong, and B.H. Lee, "Absolute strain measurements made with fiber Bragg grating sensors", *Applied Optics*, vol. 43, no. 6, pp. 1337-1341 (2004).
60. C. Shen, and C. Zhong, "Novel temperature-insensitive fiber Bragg grating sensor for displacement measurement", *Sensors and Actuators A: Physical*,

vol. 170, pp. 51-54 (2011).

61. O. M. Zepeda, S. M. Aguirre, G. B. Perez, J. C. and Mixcoatl, "Alternative interrogation method for a dual laser sensor based on fiber Bragg gratings to measure temperature using the fundamental beating frequency intensity", *Optics & Laser Technology*, vol. 67, pp. 159-163 (2015).
62. M. Sakawa, and M. Tanaka, "Introduction to Neurocomputing", Morikita Publishing Co. Ltd, pp 1-3 (1997), [In Japanese].
63. M.W. Gardner, and S.R. Dorlinga, "Artificial neural networks (the multilayer perceptron)-a review of applications in the atmospheric sciences", *Atmospheric Environment*, vol. 32, pp.2627-2636 (1998).
64. L. Rolon, S.D. Mohaghegh, S. Ameri, R. Gaskari, and B. McDaniel, "Using artificial neural networks to generate synthetic well logs", *Journal of Natural Gas Science and Engineering*, vol.1, pp. 118-133 (2009).
65. K.J. Hunt, D. Sbarbaro, R. Zbikowski, and P.J. Gawthrop, "Neural networks for control systems-A survey", *Automatica*, vol. 28, no. 6, pp. 1083-1112 (1992).
66. I. Kumazawa, "Learning and Neural network", Morikita Publishing Co. Ltd, pp 1-23 (1997), [In Japanese].
67. I. Kumazawa, "Learning and Neural network", Morikita Publishing Co. Ltd, pp 51-75 (1997), [In Japanese].
68. M. Sakawa, and M. Tanaka, "Introduction to Neurocomputing", Morikita Publishing Co. Ltd, pp 8-11 (1997), [In Japanese].
69. D. Negrov, I. Karandashev, V. Shakirov, Y. Matveyev, W. Dunin-Barkowski, and A. Zenkevich, "An approximate backpropagation learning rule for memristor based neural networks using synaptic plasticity", vol. 237, pp.193-

199 (2017).

70. S. de Montigny, "New approximation method for smooth error backpropagation in a quantron network", *Neural Networks*, vol. 60, pp.84-95 (2014).
71. K. Bahman, "Design and applications of Neural Networks", Shokodo Publishing Co. Ltd, pp 42-45 (1999), [In Japanese].
72. I.A. Basheer, and M. Hajmeer, "Artificial neural networks: fundamentals, computing, design, and application", *Journal of Microbiological Methods*, vol. 43, no.1, pp. 3-31 (2000).
73. E.T. Rolls, and S.M. Stringer, "On the design of neural networks in the brain by genetic evolution", *Progress in Neurobiology*, vol. 61, no. 6, pp. 557-579 (2000).